



Design of CMOS analog integrated circuits as readout electronics for high- T_C superconductor and semiconductor terahertz bolometric sensors



Vratislav Michal

Supervisors:

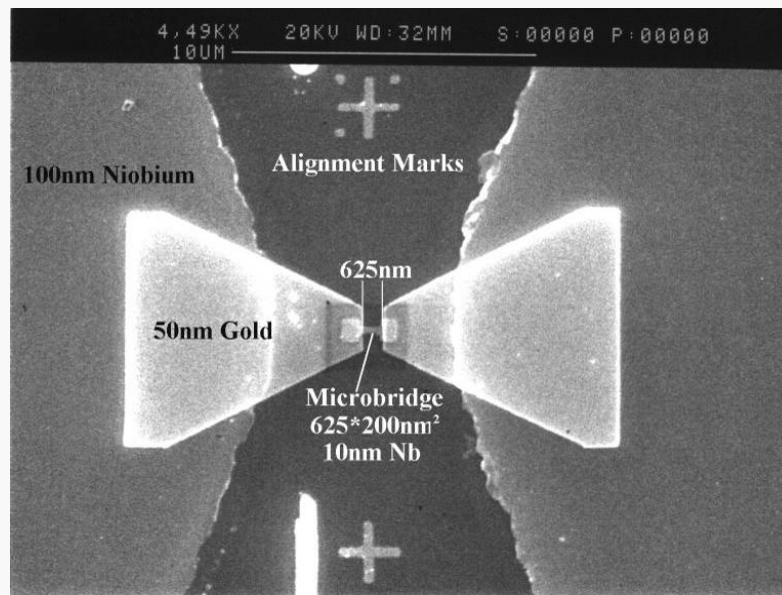
Prof. Alain Kreisler, Laboratoire de Génie Electrique de Paris-Supélec, UPMC-P6

Assoc. Prof. Jiří Sedláček, DTEEE - Brno University of Technology

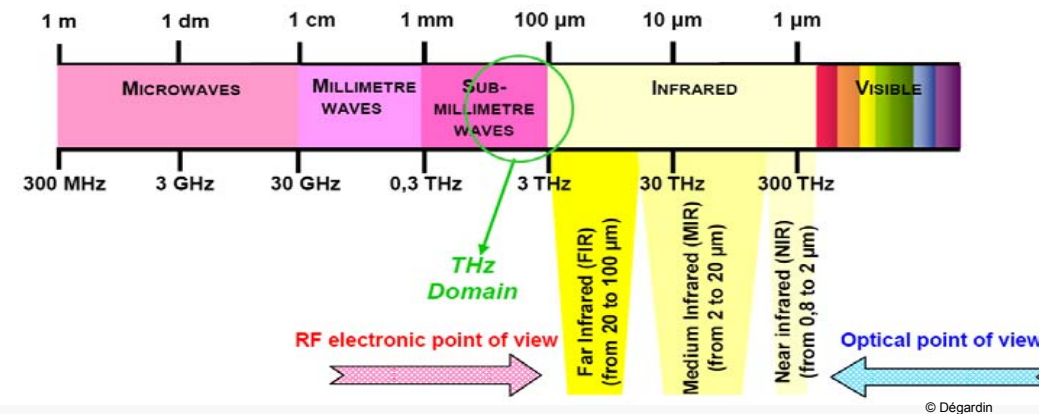
Paris, June 10th 2009



I. Introduction

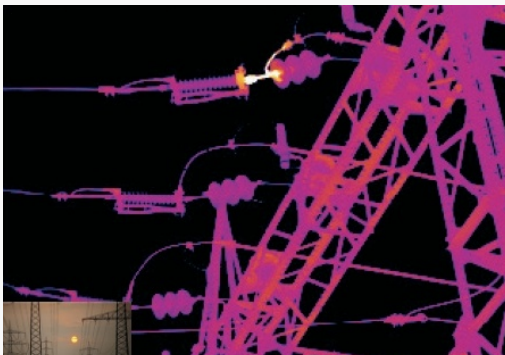


THz detection and terahertz imaging



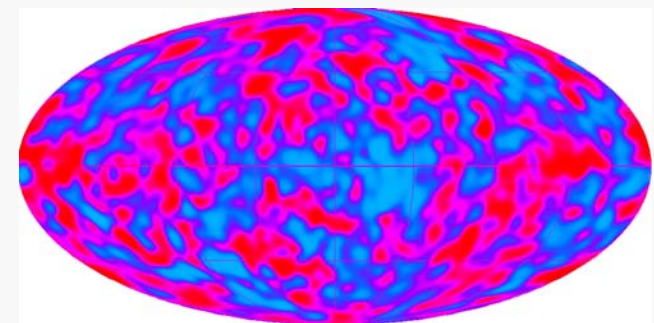
Civil application:

High voltage insulator under discharge
[\[ulis-ir website\]](#)



Research application

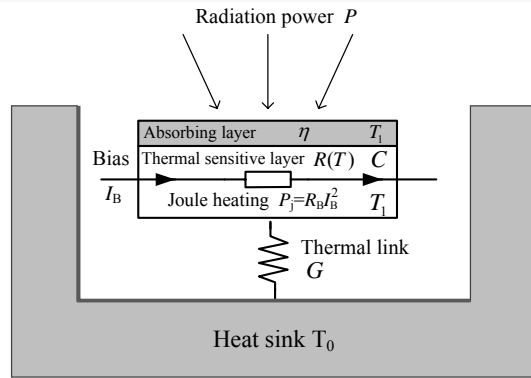
Cosmic Microwave background exploring
 (Nobel price in physic 2006)



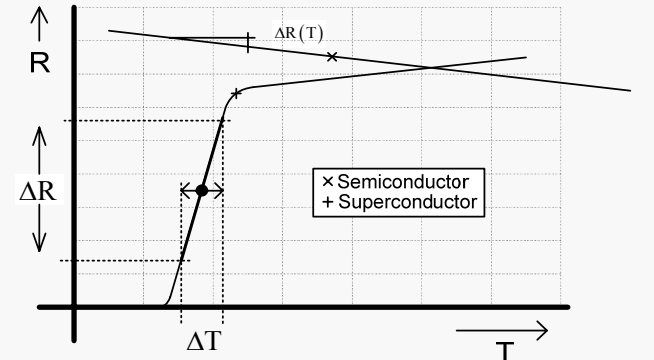
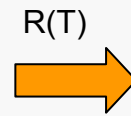
Other fields of applications:

Spectroscopy
 Civil security, medical
 Military application etc...

(THz) Bolometric detectors



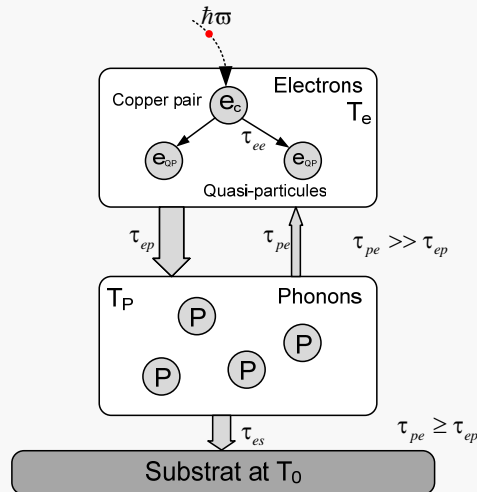
Bolometric sensor composition



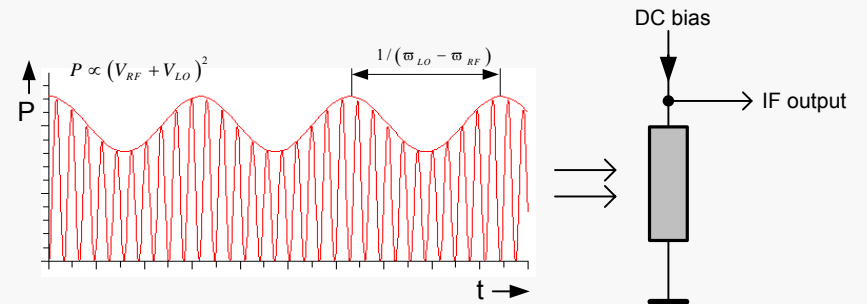
R(T) of superconductor and semiconductor

[subject of M. Aurino et M. Longhin PhD thesis]

Heterodyne detection:

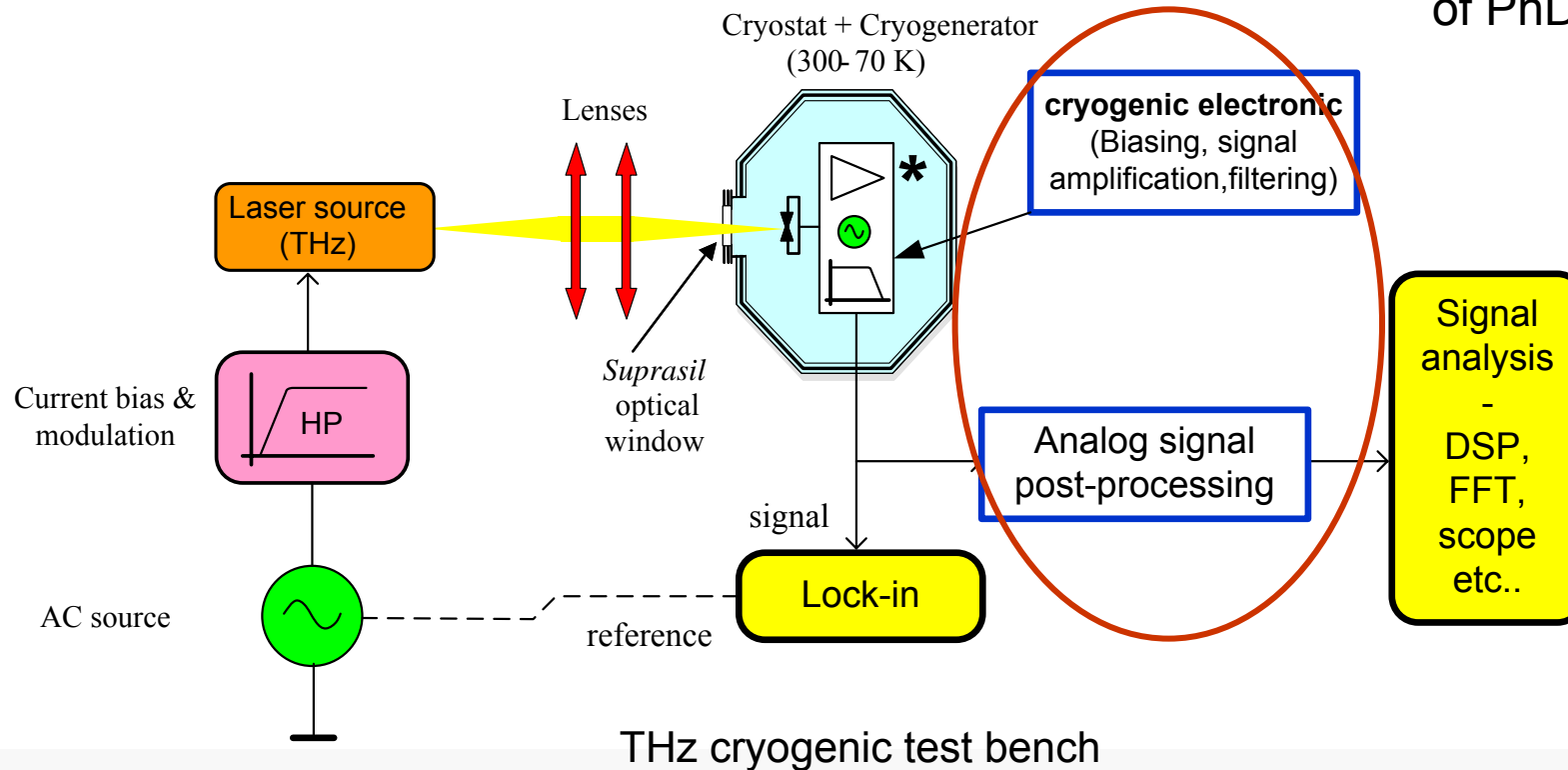


Superconducting Hot Electron Bolometer (HEB)



Characterization of new generation THz detectors: A CRUCIAL ROLE OF ELECTRONICS

blocks developed in the frame
of PhD thesis

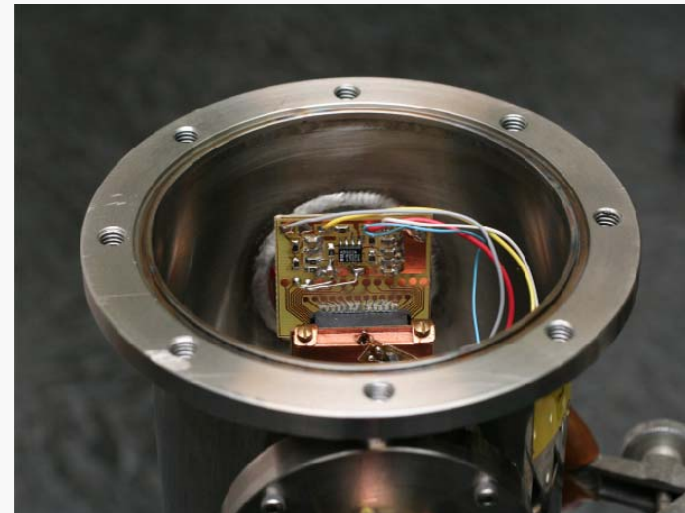
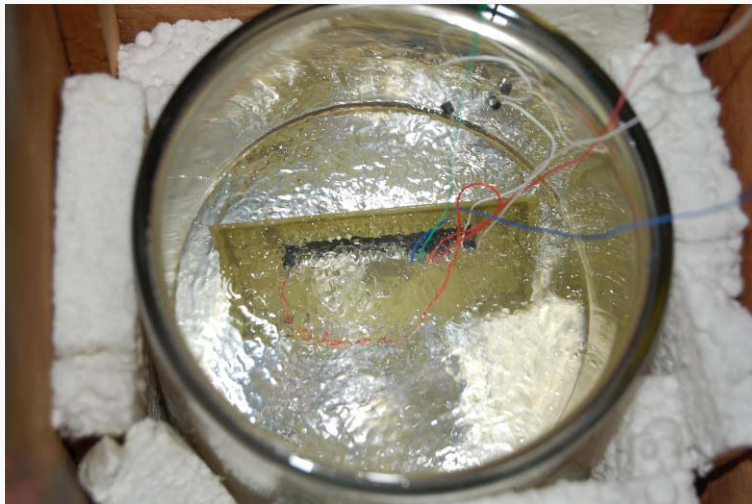


do the electronics follow up?

Research objectives of PhD thesis

- Cryogenic integrated **analog electronic** for THz detection chain
- New structures of fixed-gain CMOS **differential amplifiers** compatible with bolometric detectors at room and cryogenic temperatures
- High dynamic range signal processing:
Developpement of **frequency filters** with high attenuation rate

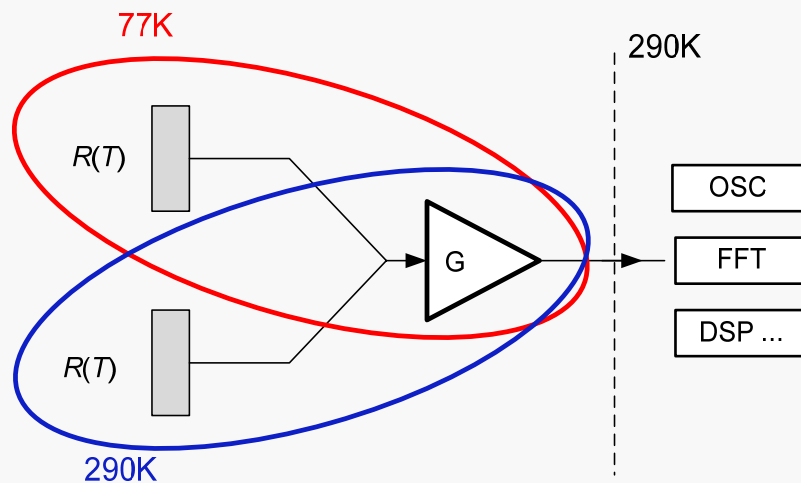
II. Differential amplifier for cryogenic instrumentation



SPECIFICATIONS

Wide temperature range CMOS differential amplifiers for:

- i) Room temperature (semiconductor bolometers)
- ii) Cryogenic temperatures (superconducting bolometers – high T_C)

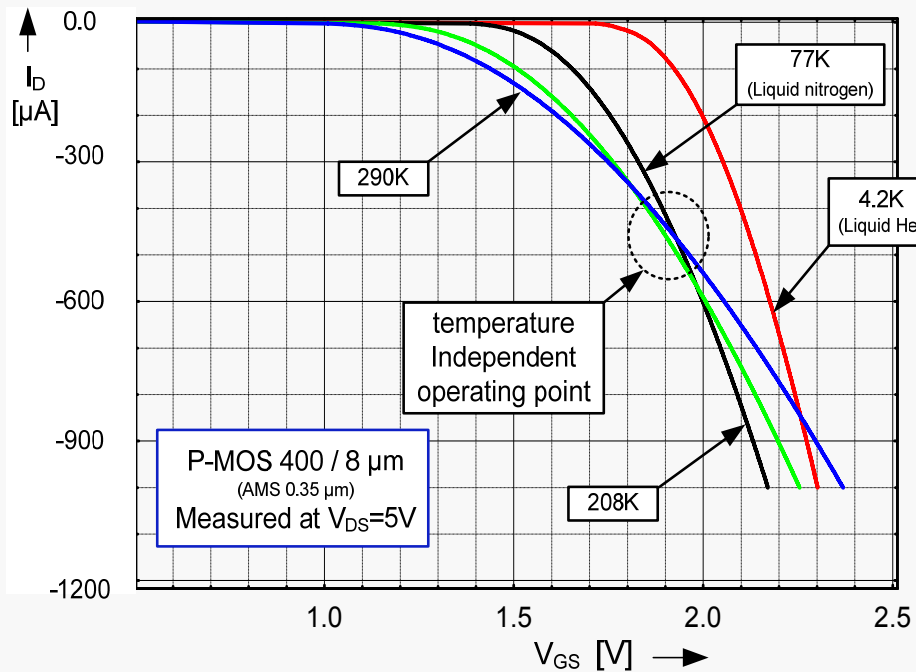


Low noise Differential CMOS amplifier

Requirements:

- 40dB, accurate gain,
- 70K to 300K temperature range,
- Differential gain BW: DC to several MHz,
- Low noise operation,
- Low power consumption
- High ($> 100k\Omega$) input impedance,
- Simple architecture.

MOS cryogenic modeling



Measured I-V characteristics for a PMOS 400/8 μm

[measurements provided in CEA-INAC laboratory in Grenoble]

→ Low field surface mobility:

$$\mu(T) = \mu(T_0) \left(\frac{T}{T_0} \right)^{-x}$$

→ Threshold voltage:

$$V_{TH}(T) = V_{TH}(T_0) [1 + \alpha_{THX} \cdot (T - T_0)]$$

→ analytical temperature model

$$I_D = \frac{KP}{2} \left(\frac{T}{T_0} \right)^{-x} \frac{W}{L} \cdot [V_{GS} - V_{TH}(T_0) [1 + \alpha_{THX} (T - T_0)]]^2$$

→ **Other effect:** Kink effect, mobility degradation
electron freeze-out

Least Square empirical model

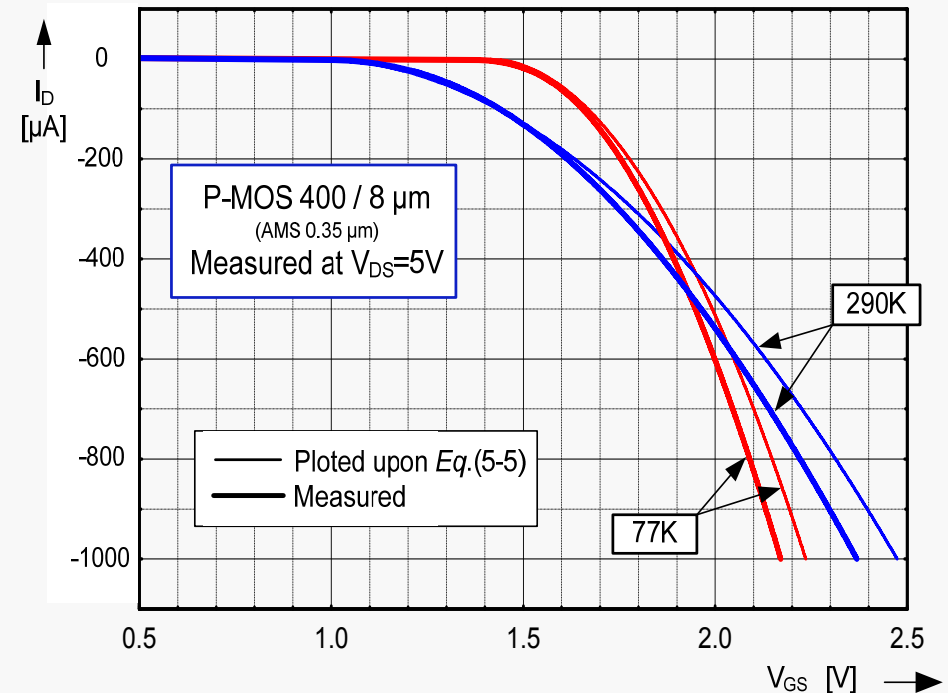
→ LM fit of $y_i = b \cdot (x_i - a)^2$:

$$R^2 \equiv \sum_{i=0}^n \left[y_i - f(x_{1,i}, x_{2,i}, \dots, x_{m,i}, a_1, a_2, \dots, a_m) \right]^2 \rightarrow \min \Rightarrow \frac{\partial R^2}{\partial a_{1,2,\dots,m}} = 0$$

Parameters based on LM fit (measurements and simulation SPICE-level 7)

TRANSISTOR	Simulation 296K	Measured 296K	Measured 77K
P-MOS 100/10μm			
KP [A/V ²]	20.67×10^{-6}	21.63×10^{-6}	72.43×10^{-6}
V _{TH} [V]	-0.9649V	-0.9534V	-1.40493V

	x	A _{THX}	V _{TH} shift
PMOS 100μm/10μm	0.90	-2.163 mK ⁻¹	-2.06 mV/K

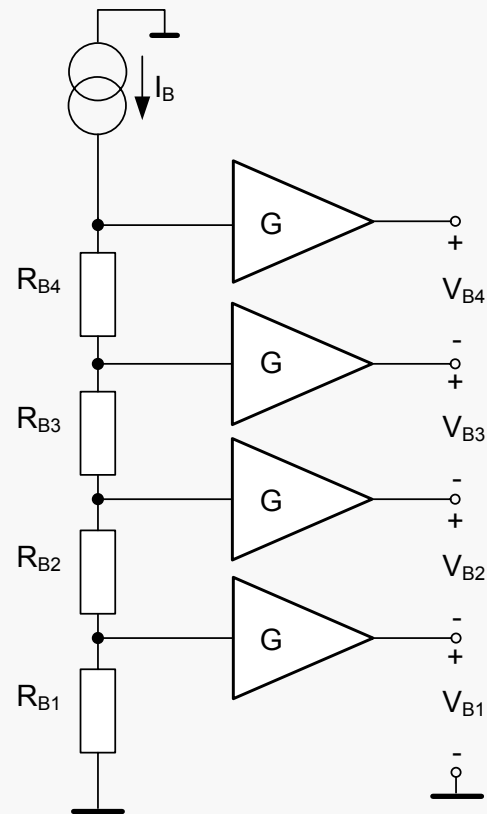


Verification of model: [different run](#)

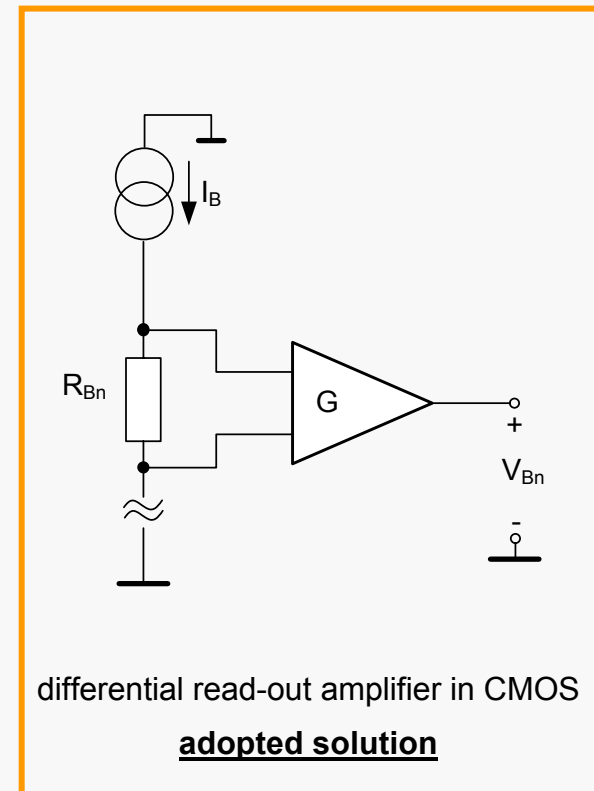
→ analytical temperature model

$$I_D = \frac{KP}{2} \left(\frac{T}{T_0} \right)^{-x} \frac{W}{L} \cdot \left[V_{GS} - V_{TH}(T_0) \left[1 + \alpha_{THX} (T - T_0) \right] \right]^2$$

DC BIAS, CONFIGURATION



Single ended amplifiers [*]



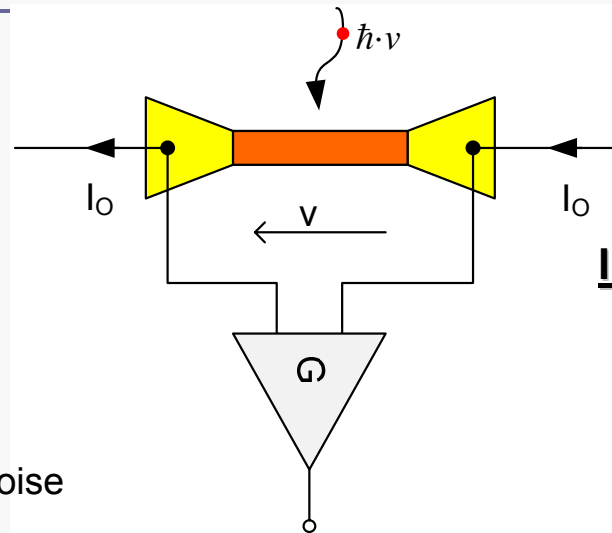
differential read-out amplifier in CMOS
adopted solution

[*] PhD thesis: F. Voisin, 2005, D. Prêle, 2006, L2E UPMC-P6

Differential amplifiers

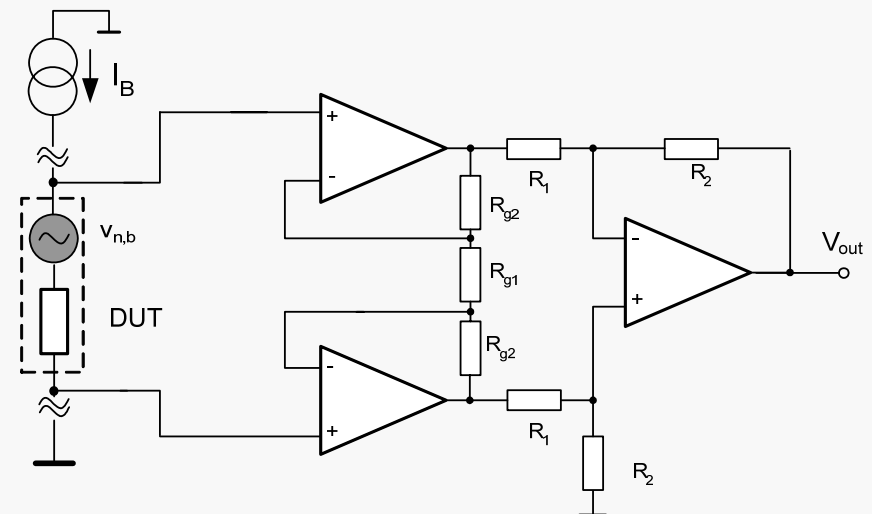
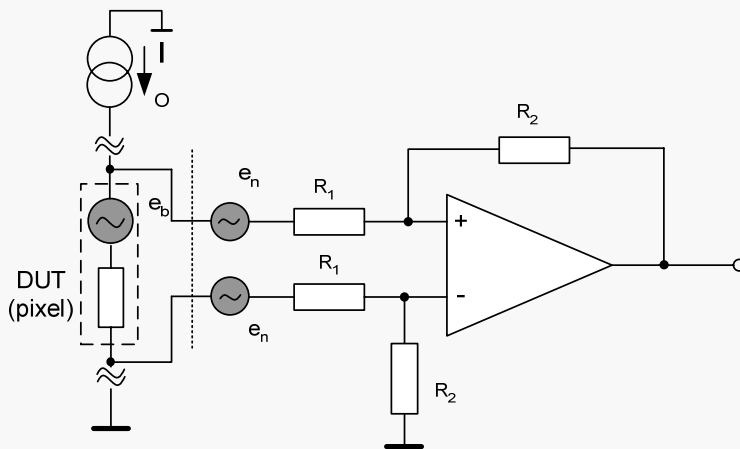
Differential OA

- Low input impedance
- High accuracy
- Higher input referred noise

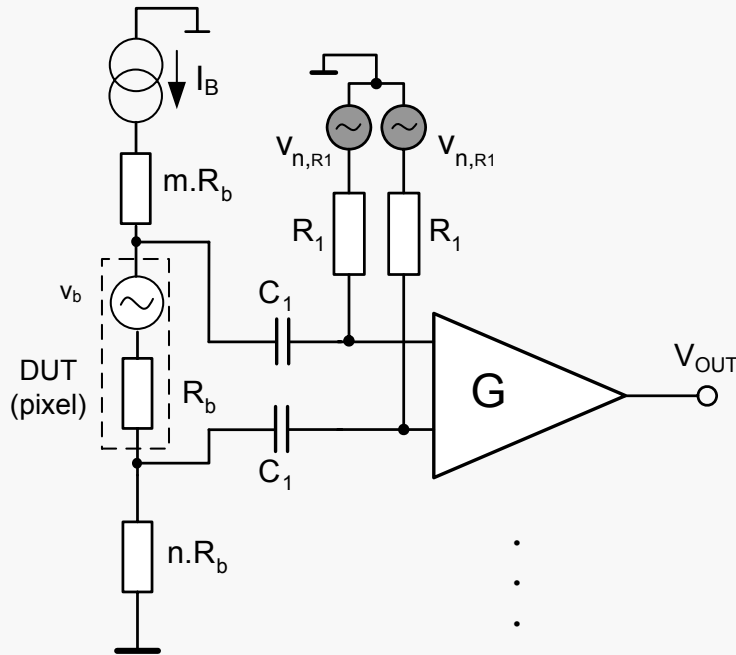


Instrumentation amplifier

- High input impedance
- Very high accuracy
- Higher input referred noise
- Low bandwidth



Solution: feedback-free amplifier

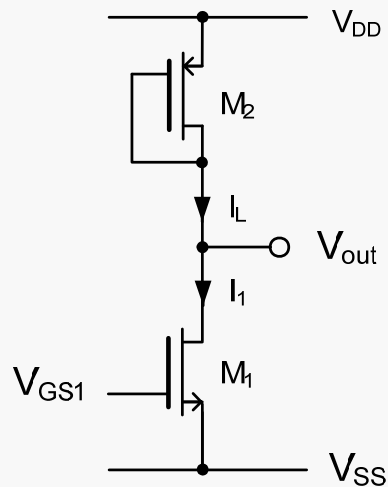


$$v_{n,in} \cong \sqrt{\frac{8k_B T}{R_1}} \cdot \left(\frac{2 + j\omega R_b C_1}{2j\omega C_1} \right) *$$

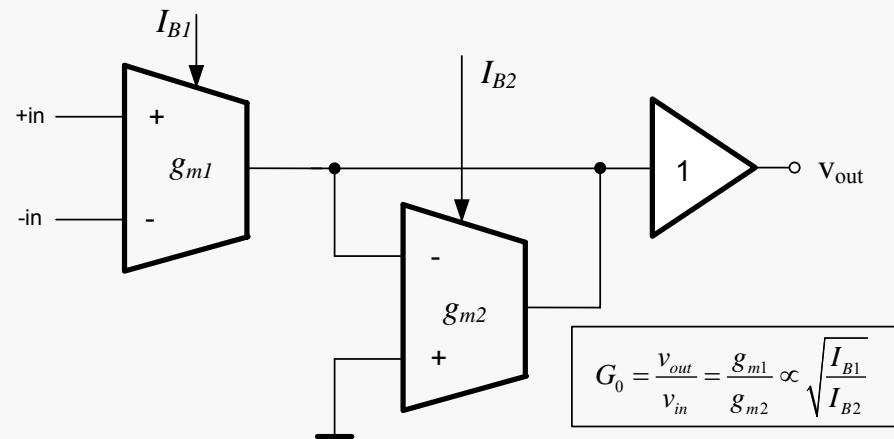
* Bolometer noise voltage is neglected

- ☺ **No resistors in the structure**
 → simplification, reduced noise, and I_q, silicon surface save
- ☺ **Absence of compensation**
 → improves time characteristics (no stability problems) and allows to reach higher BW
- ☹ **Linearity, distortion**
- ☹ **Missing experiences and developed architectures in bipolar and CMOS**

Known structures – low gain



Common source MOS amplifier



OTA Amplifier differential fixed-gain amplifier

The expression of the gain follows a square-root law:

$$G_0 = \frac{dV_{OUT}}{dV_{GS1}} = -\sqrt{\frac{KP_N}{KP_P}} \sqrt{\frac{W_1/L_1}{W_2/L_2}}$$



For 40 dB, the $(W/L)_1 / (W/L)_2$

as high as $10\,000 \cdot KP_P / KP_N$

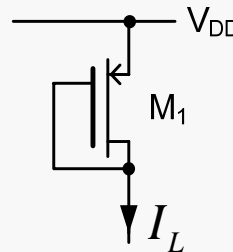
Adopted technique: low g_m load

Voltage gain fixed in the structure by the transconductance ratio

Voltage output is created by the voltage buffer

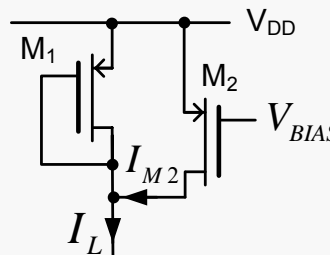
Active loads

MOS diode



$$g_m = \sqrt{2KP \frac{W}{L} I_L}$$

Decreasing the transconductance by current sink [PhD F. Voisin, 2005]

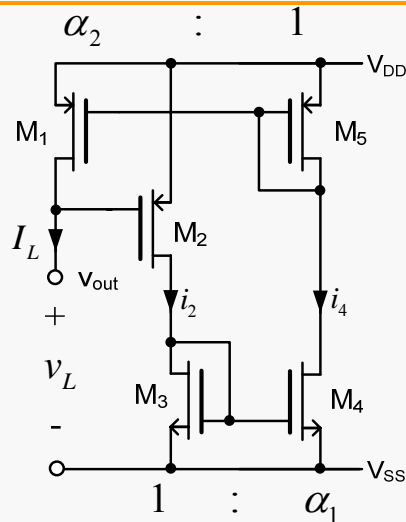


$$g'_m = \sqrt{2KP \cdot \frac{W_1}{L_1} (I_L - I_{M2})}$$

Current difference makes the function very sensitive:

$$S_k^{g'_m} = \frac{\partial g'_m(k)}{\partial k} \cdot \frac{k}{g'_m(k)} = -\frac{1}{2} \frac{k}{1-k}$$

Proposed low g_m composite transistor



Proposed method for decreasing the transconductance by means of **current scaling:**

$$g'_m = \sqrt{2 \cdot KP_{(T_2)} \cdot \frac{W_2}{L_2} \cdot \left(\frac{\frac{W_4 \cdot W_1}{L_4 \cdot L_1}}{\frac{W_3 \cdot W_5}{L_3 \cdot L_5}} \right)} \cdot I_L$$



Inaccurate

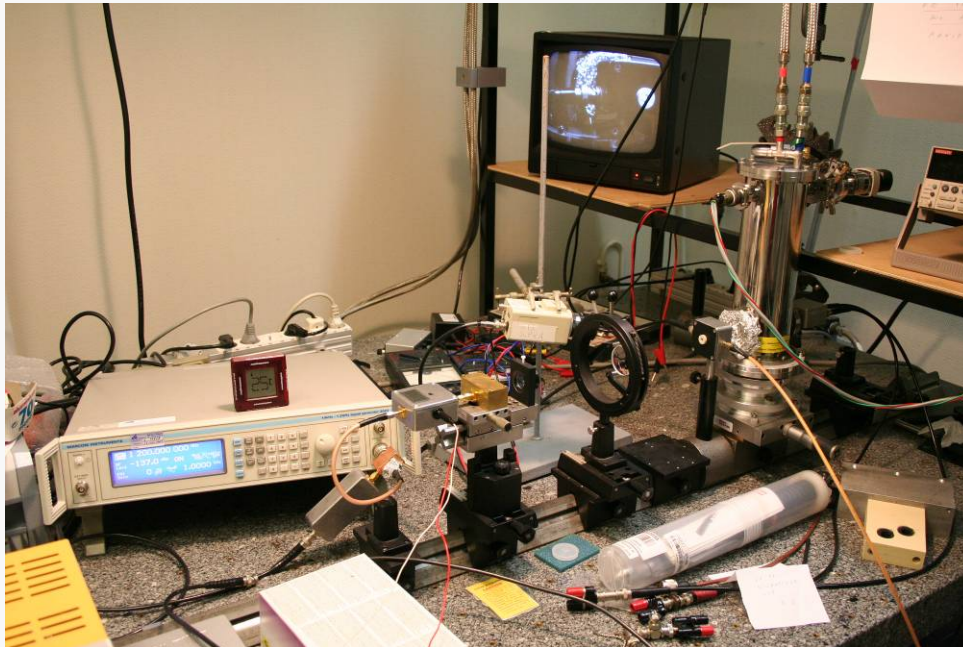
accurate



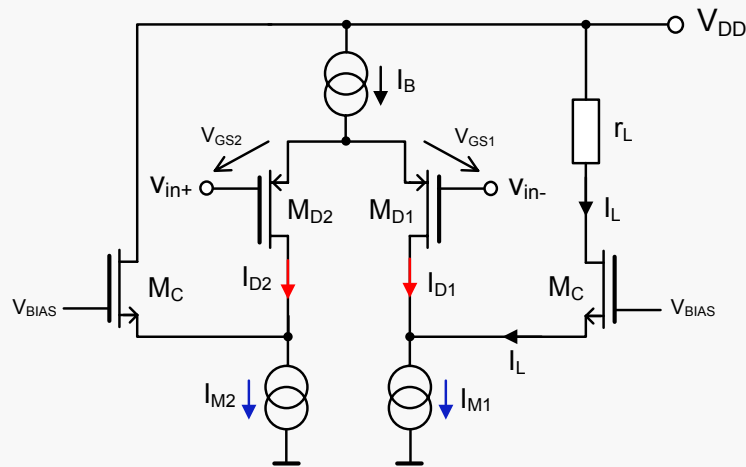
$$g'_m = \frac{i_L}{v_L} = g_{m2} \cdot \frac{g_{m4} \cdot g_{m1}}{g_{m3} \cdot g_{m5}} = \alpha_1 \cdot \alpha_2 \cdot g_{m2}$$

II.1

1st folded cascode amplifier



Folded cascode OTA: analysis



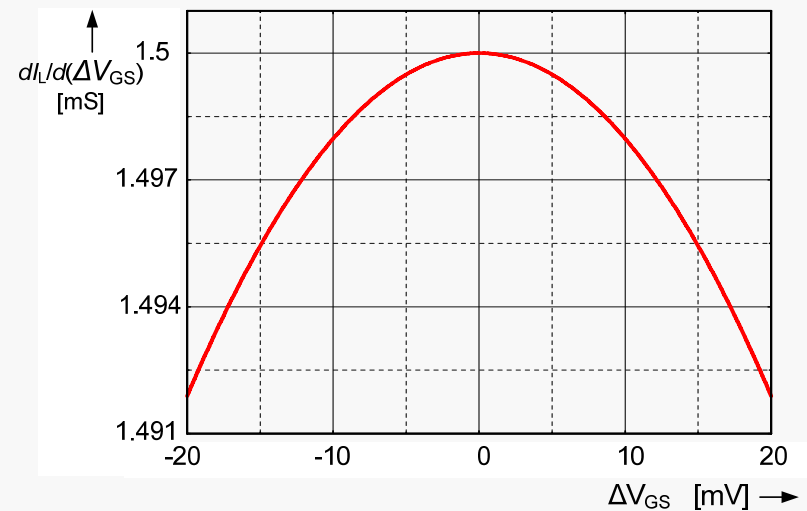
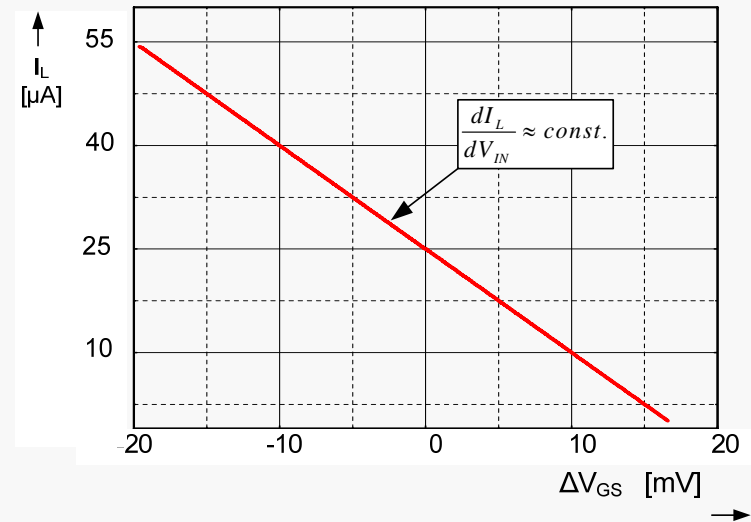
→ DC characteristic:

$$I_{D1} = \frac{1}{8} \cdot \left(\sqrt{4 \cdot I_B - KP \cdot \frac{W_D}{L_D} \cdot \Delta V_{GS}^2} + \sqrt{KP \cdot \frac{W_D}{L_D} \cdot \Delta V_{GS}^2} \right)^2$$

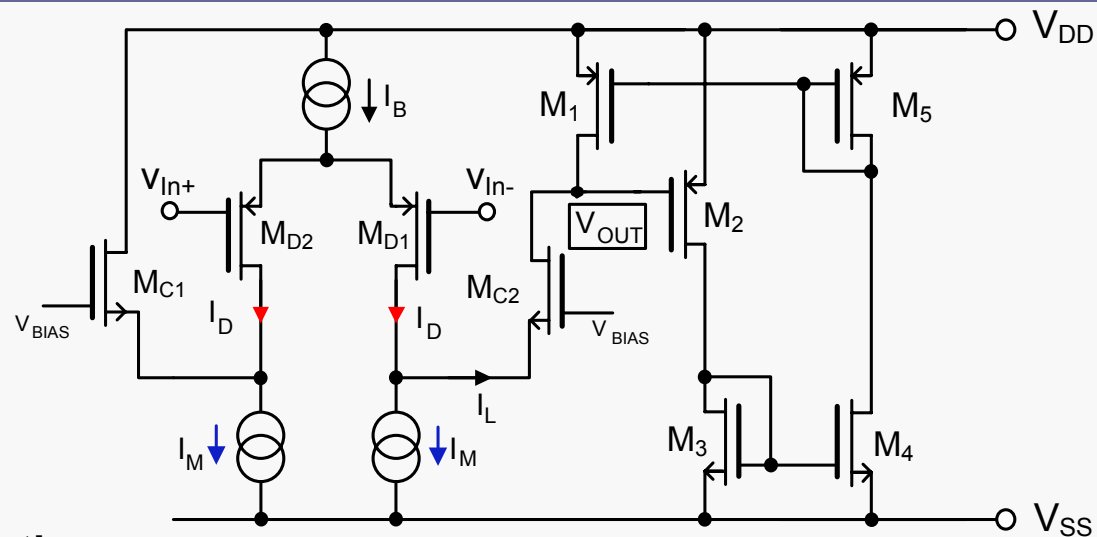
→ g_m :

$$g_{mDiff} = \left. \frac{dI_{D1}}{d\Delta V_{GS}} \right|_{\Delta V_{GS}=0} = \frac{1}{2} \cdot \sqrt{KP_P \cdot \frac{W_D}{L_D} \cdot I_B}$$

For required input voltage range, the stage behaves as quasi-linear current source



Proposed 1st folded cascode amplifier



➤ DC transfer characteristic:

$$V_{OUT} = V_{DD} - |V_{TH,P}| - \sqrt{\frac{2}{K_{P_p} \cdot \left(\frac{W_2}{L_2}\right)} \cdot \left(\frac{W_3 \cdot W_5}{L_3 \cdot L_5}\right) \cdot \left(\frac{W_4 \cdot W_1}{L_4 \cdot L_1}\right)} \cdot \left[I_{M1} - \frac{1}{8} \cdot \left(\sqrt{4 \cdot I_B - K_{P_p} \cdot \frac{W_D}{L_D} \cdot \Delta V_{GS}^2} + \sqrt{K_{P_p} \cdot \frac{W_D}{L_D} \cdot \Delta V_{GS}} \right)^2 \right]$$

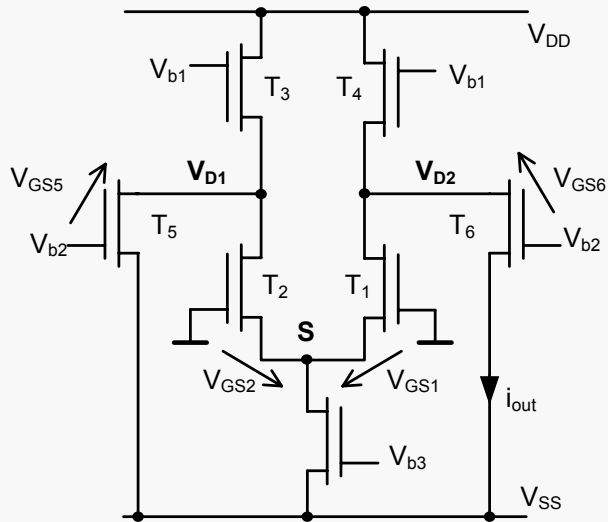
➤ Gain is the slope of DC transfer characteristic:

$$G_0 = \left. \frac{dV_{out}}{d\Delta V_{GS}} \right|_{\Delta V_{GS}=0} = \frac{1}{2} \sqrt{\frac{L_{eff}}{W_{eff}} \cdot \frac{W_D}{L_D}} \cdot \sqrt{\frac{I_B}{2 \cdot I_{L(\Delta V_{GS}=0)}}},$$

where:

$$\frac{W_{eff}}{L_{eff}} = \frac{W_2 \cdot W_4 \cdot W_1}{L_2 \cdot L_4 \cdot L_1} \cdot \frac{L_3 \cdot L_5}{W_3 \cdot W_5}$$

Noise analysis of folded cascode

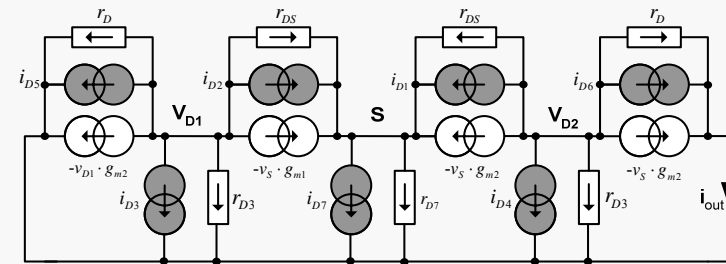


The equivalent input noise:

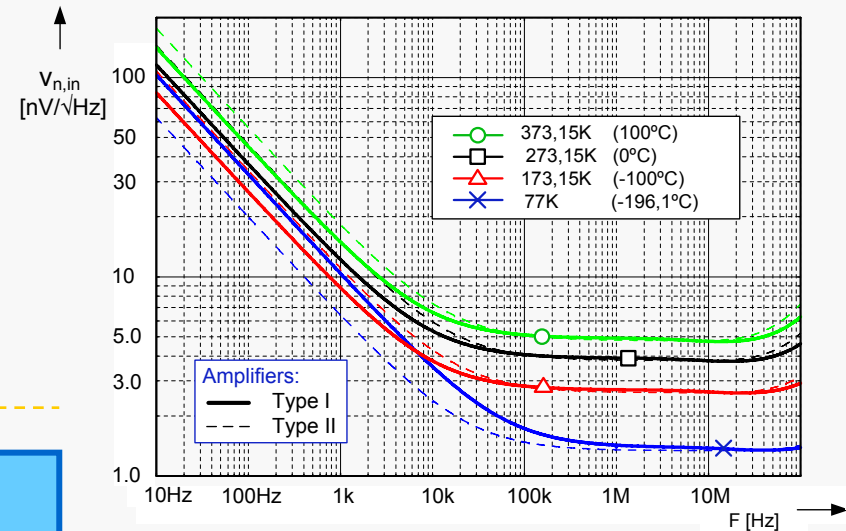
$$\bar{e}_{in}^2 = \frac{\bar{e}_{OUT}^2}{G^2} = \frac{8}{3} k_B T \left(\frac{1}{2} \cdot \frac{1}{g_{m\text{diff}}} + \frac{1}{4} \cdot \frac{g_{m7}}{g_{m\text{diff}}^2} + \frac{g_{m4}}{g_{m\text{diff}}^2} \right)$$

A very low thermal noise is observed at cryogenic temperature ($T = 77 \text{ K}$):

$$v_{n,\text{in}} = 1.5 \text{ nV}/\sqrt{\text{Hz}}$$

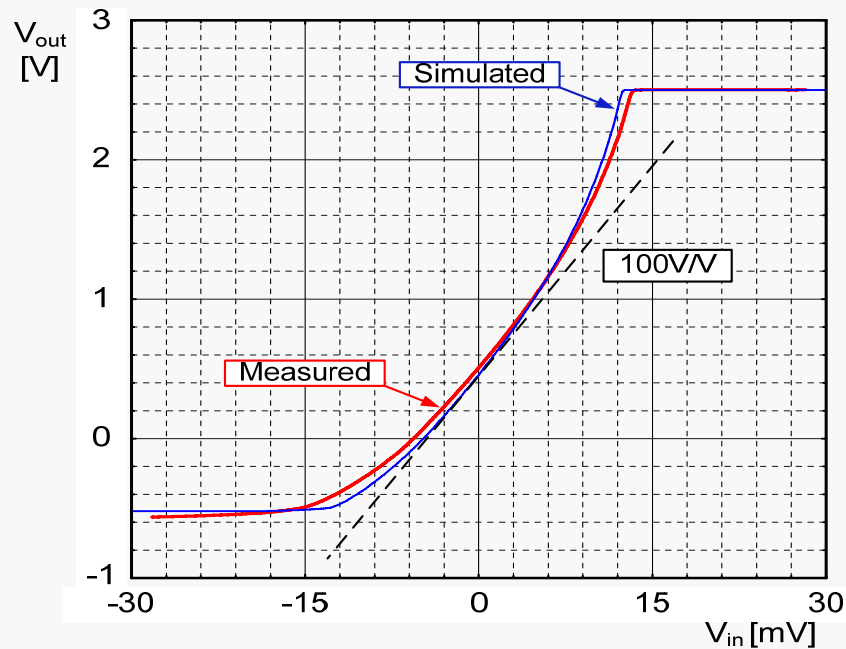


Small signal equivalent circuit.

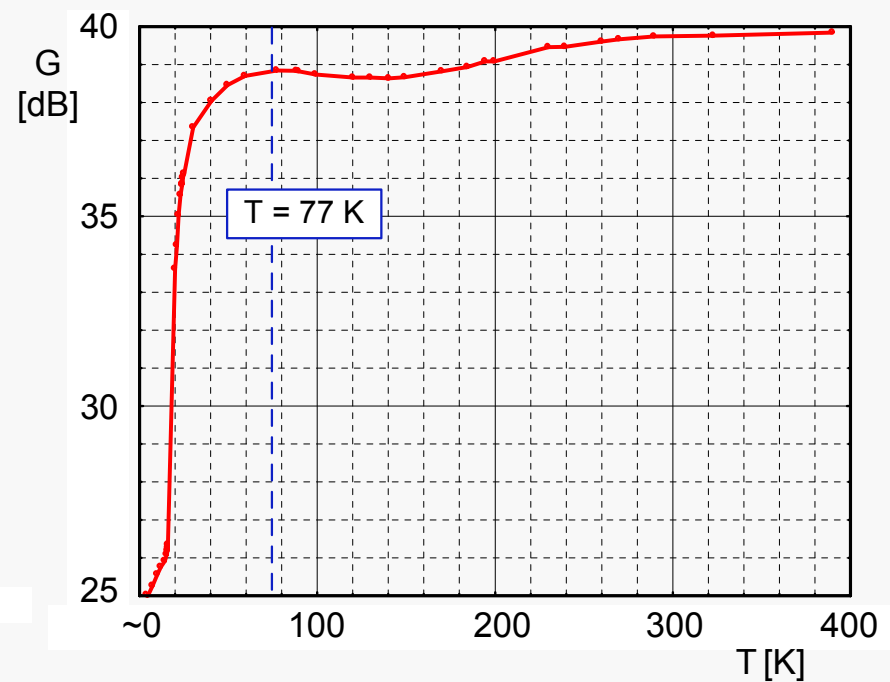


Simulated input-referred noise voltage (both amplifiers)

Measurements: wide temperature results



DC transfer characteristic at 290K

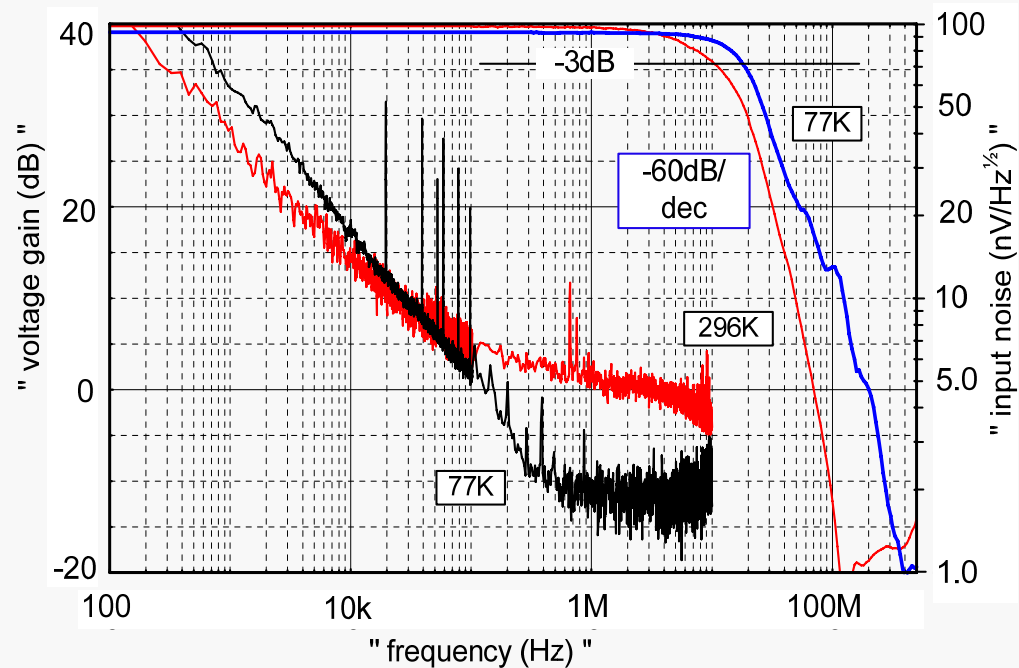


Temperature function of voltage gain

Results DC and AC characteristics

Amplifier	Gain [dB]
A_5	39.84
A_{5_2}	39.75
A_1	40.10
A_2	39.62
A_3	39.52
A_4	39.85
AVG	39.78

Dispersion of voltage gain
(A_{5_2} refers to chip 2)

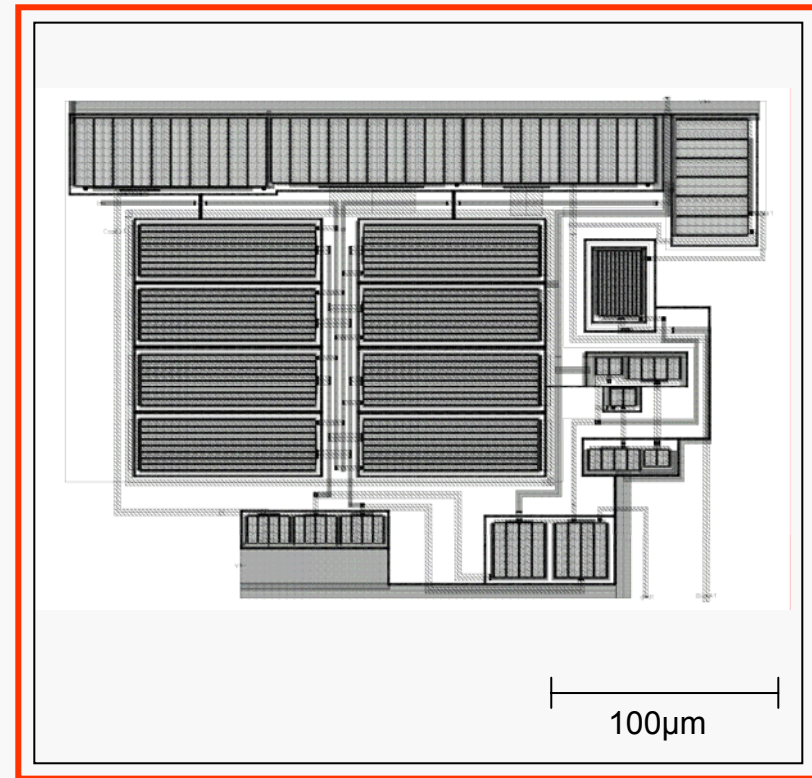


AC response and input noise ($V_{DD}=5V$, $I_Q=2mA$)



1st amplifier: summary

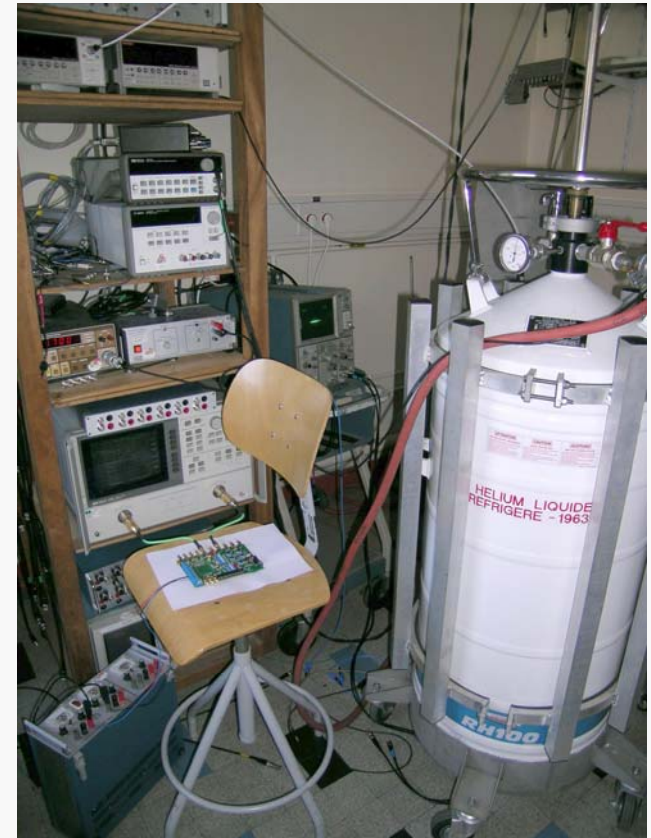
- **New amplifier architecture for extreme temperature range**
- **State-of-the art: low noise and large BW operation (up to 1.7GHz GBW at $I_q = 2.1\text{mA}$)**
- **Gain is fixed by means of geometric ratio: no variation with temperature**
- **Sufficient linearity for small signals: DC characteristic $\propto \sqrt{V_{in}}$**



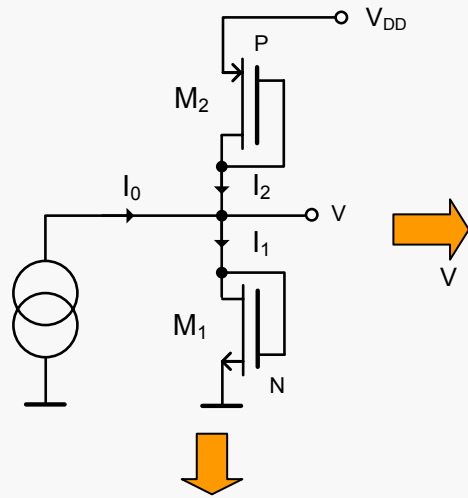
Layout in CMOS 0.35µm AMS process

II.2

2st amplifier: linearization and temperature compensation

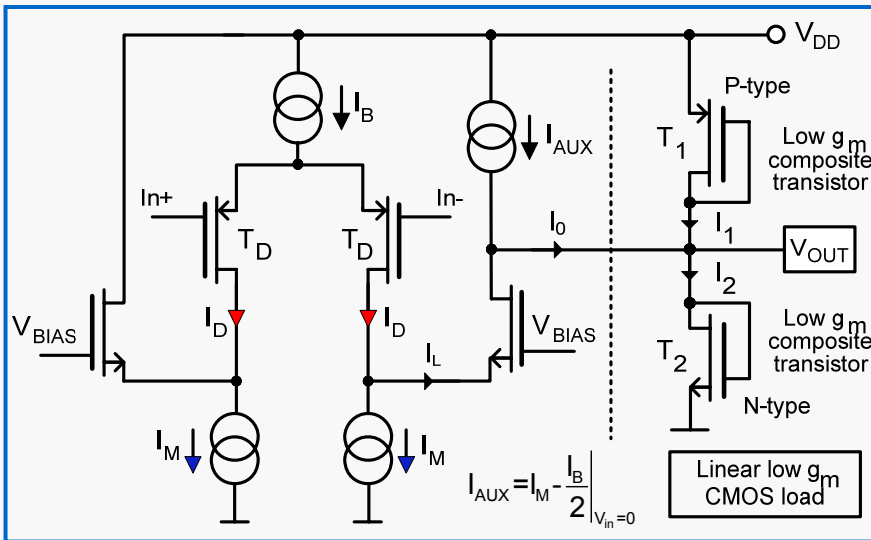


2nd amplifier: new temperature compensation and linearization



Based on **cancelling the quadratic terms**. The node equation can be written:

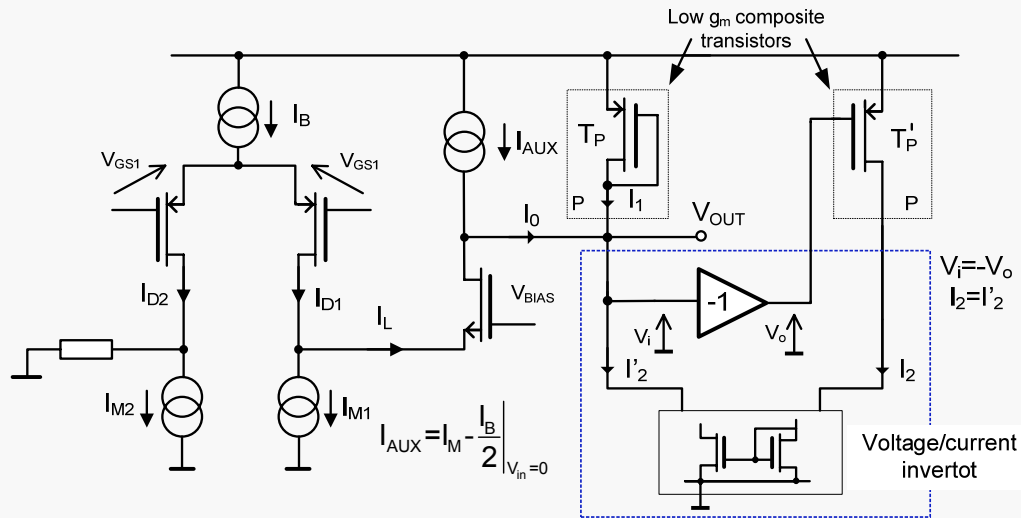
$$\frac{\beta_1}{2} (V - V_{TH1})^2 = \frac{\beta_2}{2} (V_{DD} - V - |V_{TH2}|)^2 + I_0$$



The extraction of output voltage leads to (assuming $\beta_1 = \beta_2$, $V_{TH1} = V_{TH2}$):

$$V = \frac{V_{DD}}{2} + \frac{I_0}{\beta(V_{DD} - 2 \cdot |V_{TH}|)}$$

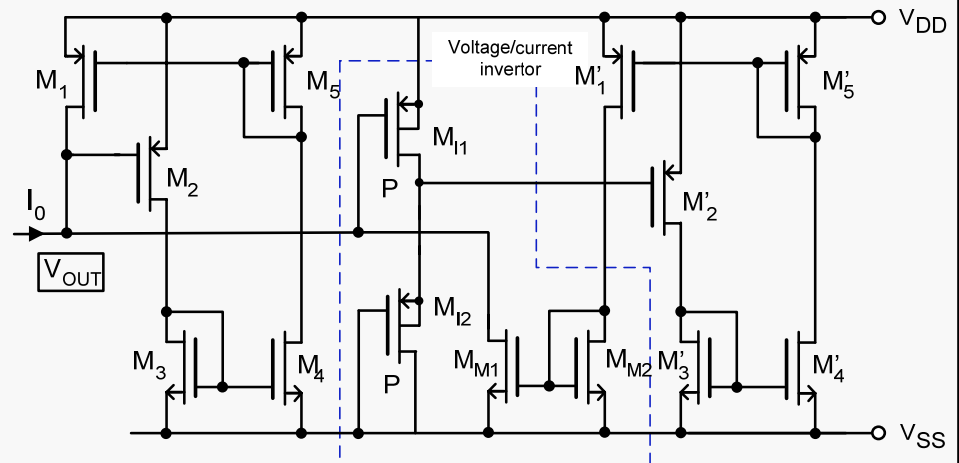
Condition: $\beta_1 = \beta_2$, $V_{TH1} = V_{TH2}$: solution



← Symmetrisation of the low g_m linear load

Single well

→ Symmetric low- g_m CMOS load →



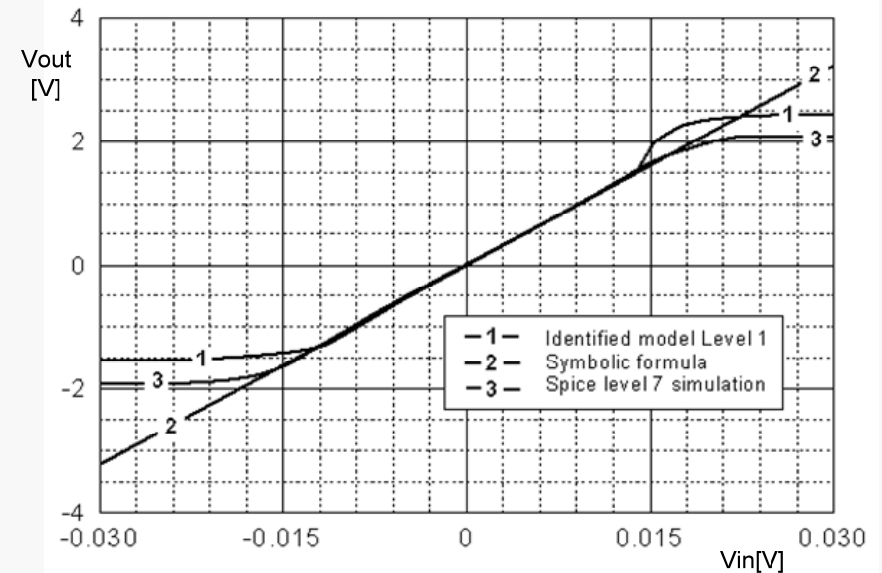
Analysis of DC transfer

→ DC transfer function:

$$V_{out} = \frac{1}{2}V_{DD} + \frac{\frac{1}{2}I_B - \frac{1}{8}\left(\sqrt{4 \cdot I_B - KP_P \cdot \frac{W_D}{L_D} \cdot \Delta V_{GS}^2} + \sqrt{KP_P \cdot \frac{W_D}{L_D} \cdot \Delta V_{GS}}\right)^2}{KP_P \cdot \frac{W_{eff}}{L_{eff}} \cdot (V_{DD} - 2 \cdot |V_{TH,P}|)}$$

→ Gain is given by derivation:

$$G_0 = \left. \frac{dV_{out}}{d\Delta V_{GS}} \right|_{\Delta V_{GS}=0} = \frac{1}{2} \cdot \frac{\sqrt{I_B \cdot \frac{W_D}{L_D}}}{\sqrt{KP_P} \cdot \frac{W_{eff}}{L_{eff}} \cdot (V_{DD} - 2 \cdot |V_{TH,P}|)}$$



DC transfer characteristics

The voltage gain as the function of:

- $\sqrt{(W/L)_D/(W/L)_{eff}}$ ratio,
- Technological parameters: $\sqrt{KP_P}$, $V_{TH,P}$.
- Bias current I_B and power supply voltage V_{DD} .

	KP	V_{TH}	V_{DD}	I_B	W_D/L_D	$\frac{W_{eff}}{L_{eff}}$
$S_{x_i}^G$	$-\frac{1}{2}$	$\frac{2 \cdot V_{THP}}{V_{DD} - 2 \cdot V_{THP}}$	$-\frac{V_{DD}}{V_{DD} - 2 \cdot V_{THP}}$	$\frac{1}{2}$	$\frac{1}{2}$	-1

Temperature compensation principle: current / voltage biasing

→ Gain is given by derivation:

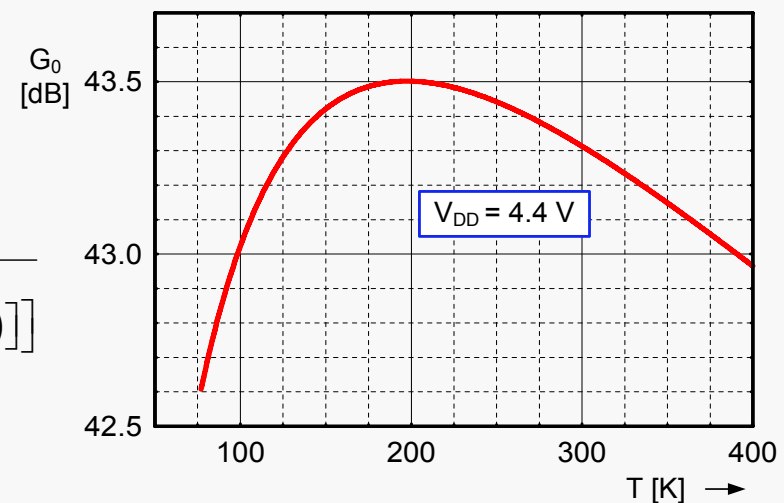
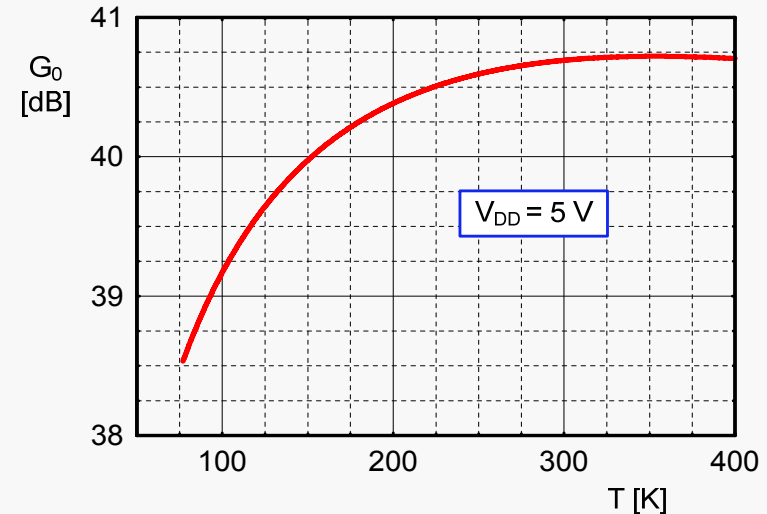
$$G_0 = \left. \frac{dV_{out}}{d\Delta V_{GS}} \right|_{\Delta V_{GS}=0} = \frac{1}{2} \cdot \frac{\sqrt{I_B \cdot \frac{W_D}{L_D}}}{\sqrt{KP_P} \cdot \frac{W_{eff}}{L_{eff}} \cdot (V_{DD} - 2 \cdot |V_{TH,P}|)}$$

→ We replace the elements without temperature dependence by C:

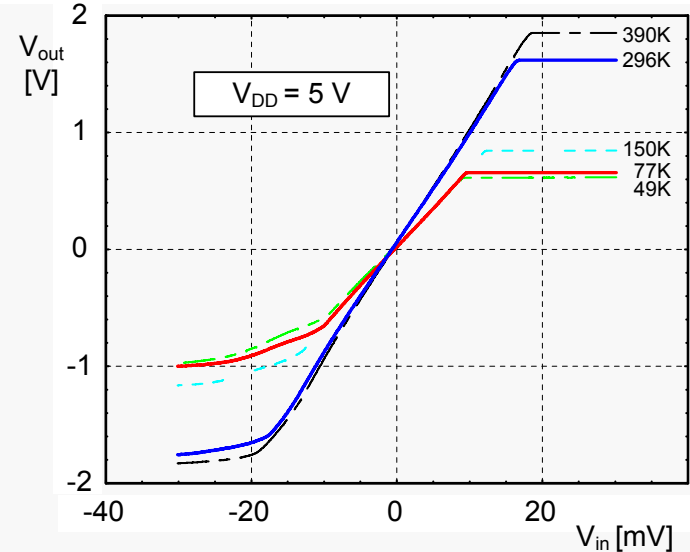
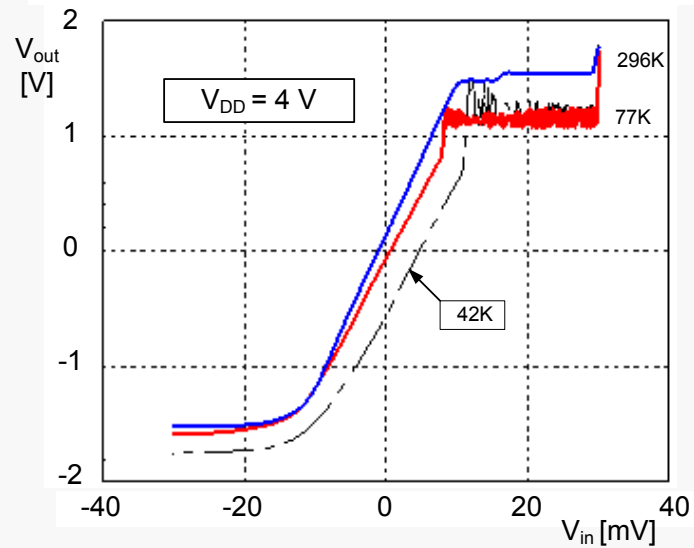
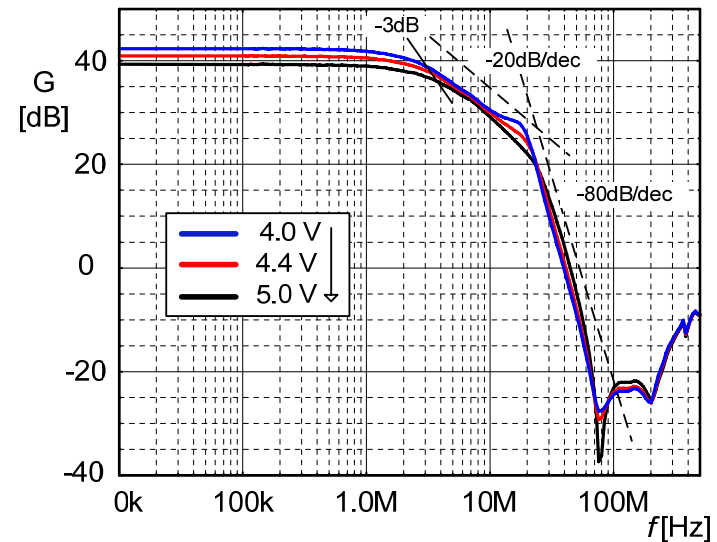
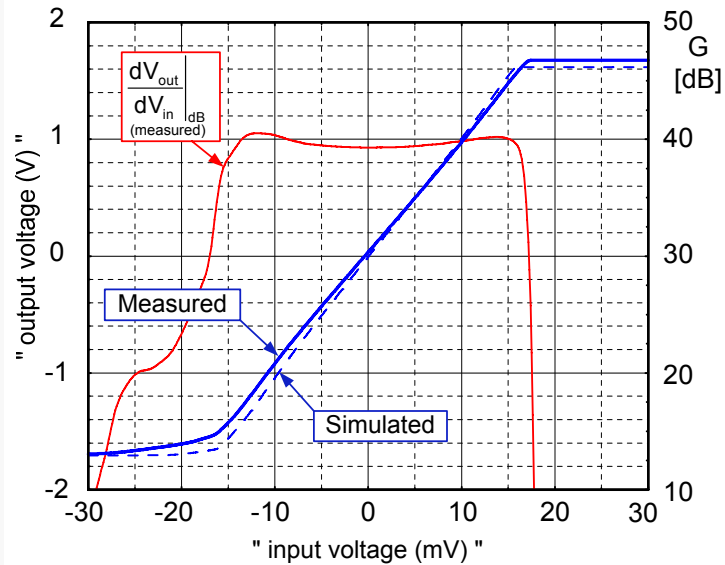
$$G_0(T) = \frac{C}{\sqrt{KP_P(T)} \cdot (V_{DD} - 2 \cdot |V_{TH,P}(T)|)}$$

→ Which leads to:

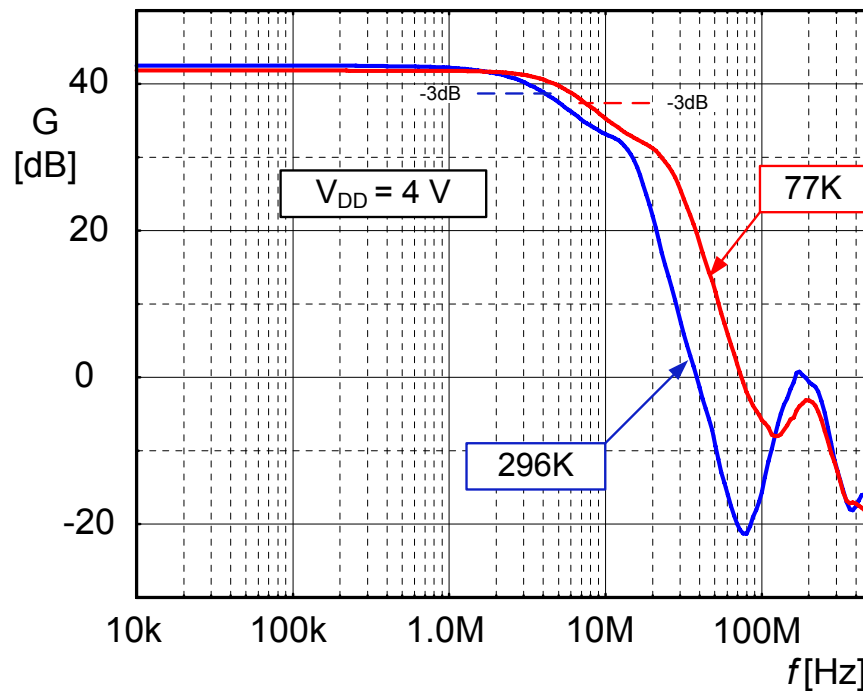
$$\frac{G_0(T)}{C} = \frac{1}{\sqrt{KP_P(T_0)} \cdot \left(\frac{T}{T_0}\right)^{-x} \cdot [V_{DD} - 2 \cdot |V_{TH,P}(T_0)| [1 + \alpha_{THX} \cdot (T - T_0)]]}$$



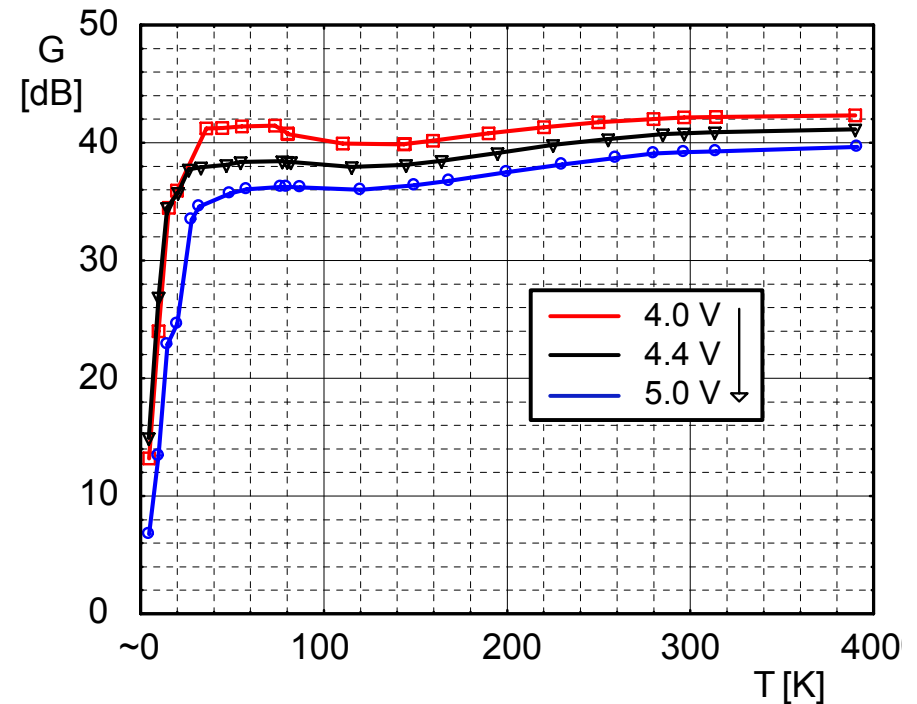
Measurements: wide temperature results



Measurements: wide temperature results



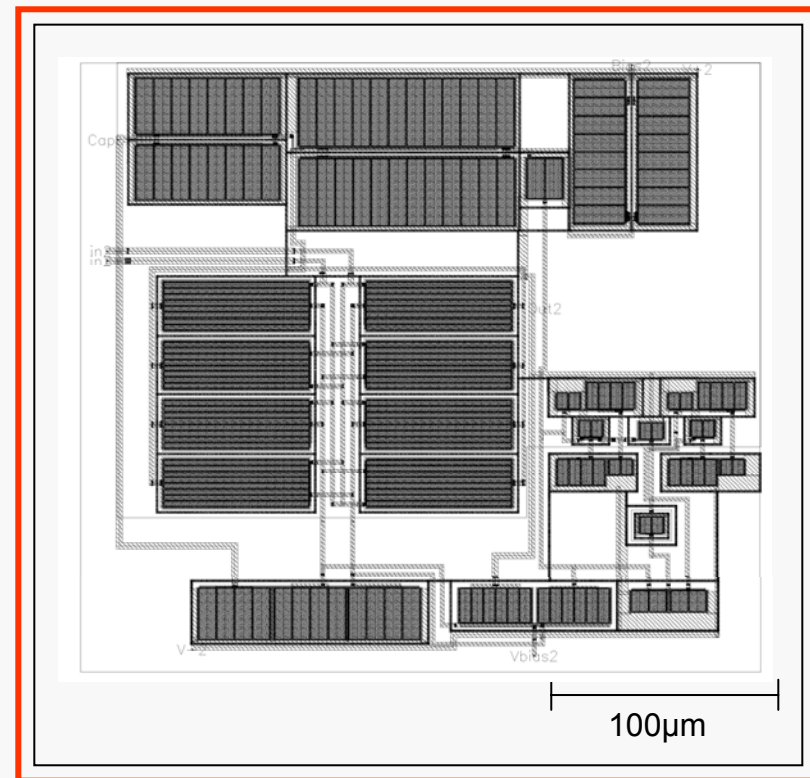
AC transfer @ 2.5V, 290 and 77 K



Temperature gain junction for three VDD voltages

2st amplifier: summary

- New **amplifier architecture** for extreme temperature range
- Wide **linear** operation
Temperature compensation
- Low noise, wide BW achieved with low I_q (Up to **1GHz GBW** for 1.3mA quiescence current)
- **Highly competitive** to bipolar amplifier, promising as compact block for VLSI integration



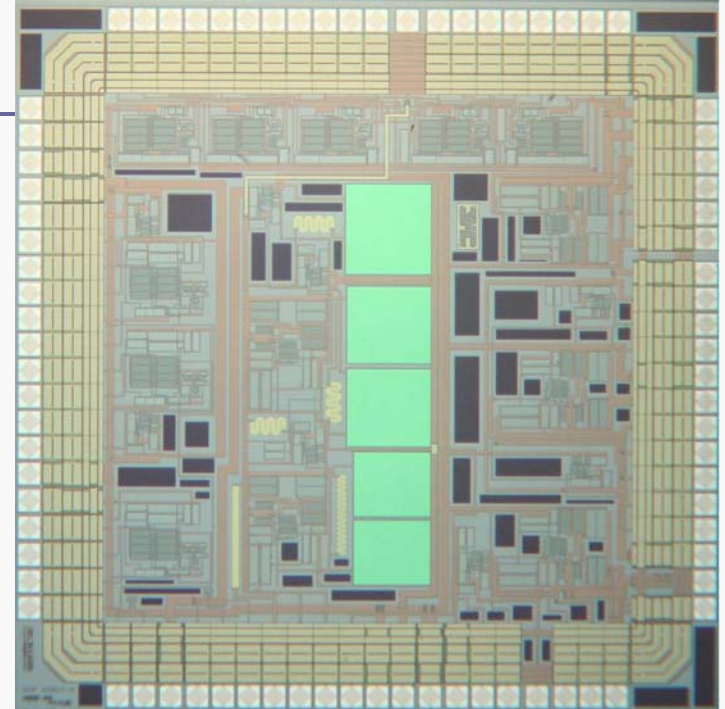
Layout in CMOS 0.35µm AMS process

V. Michal et al. "Fixed-gain CMOS differential amplifiers with no external feedback for a wide temperature range", Cryogenic (2009), [doi:10.1016/j.cryogenics.2008.12.014](https://doi.org/10.1016/j.cryogenics.2008.12.014)

Comparison with industrial state of the art

Key parameters of developed amplifiers

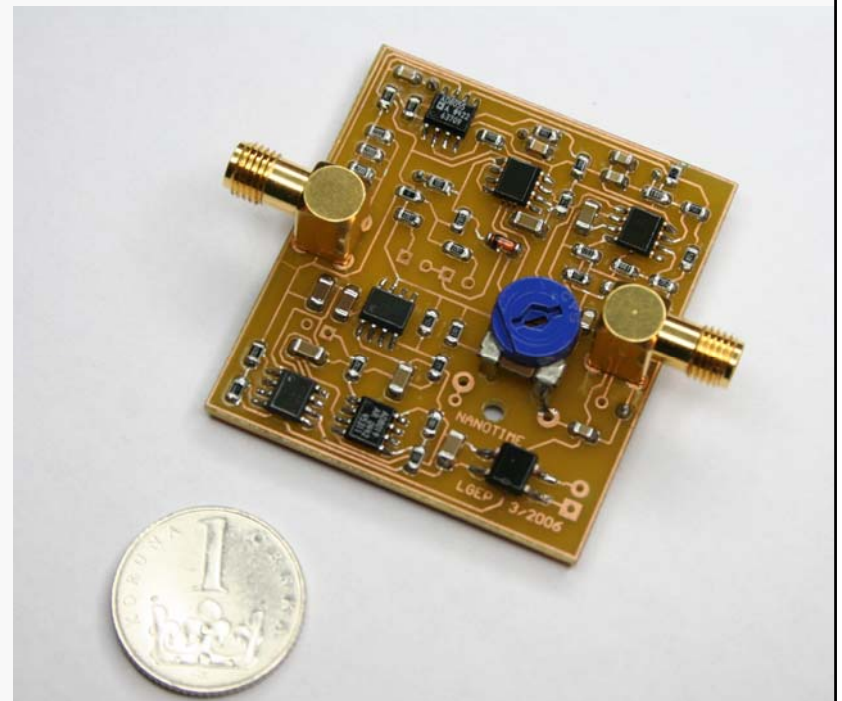
MEASURED PARAMETERS	TYPE I AMPLIFIER	TYPE II AMPLIFIER
Operating supply voltage	4.1 V to 5.5 V	3.6 V to 5.5 V
Quiescent current	2.1 mA	1.3 mA
-3 dB bandwidth (T = 290 K)	10 MHz (GBW=1GHZ)	4 MHz at V _{DD} = 5 V
-3 dB bandwidth (T = 77 K)	17 MHz (GBW=1.7GHZ)	10 MHz at V _{DD} = 5 V
Input noise (T = 290 K)	5 nV/Hz ^{1/2}	5 nV/Hz ^{1/2}
Input noise (T = 77 K)	2 nV/Hz ^{1/2}	3 nV/Hz ^{1/2}
Gain G ₀ (T = 290 K)	39.85 dB	39.3 dB at V _{DD} = 5 V
Δ Gain 270 K - 390 K	-0.12 dB	-0.5 dB at V _{DD} = 4 V
Gain error (at T = 77 K)	-1.2 dB	-1.3 dB at V _{DD} = 4 V
THD ² (V _{out} = 0.3 V _{pp})	1 %	0.03 %



Industrial differential amplifiers (room temperature)

Type	Configuration	GBW [MHz]	SR [μV/s]	VDD [V]	I _q [mA]	Input noise nV/√Hz	Other
AD8045	OA Bipolar	1000	1350	3.3 - 12	19 × 3	3	
LTC6401-20	Fixed gain 20dB+/-0,6dB Bipolar	1300	4500	2,85-3,5	50 × 3	2,1	R _{in} =200Ω
LT1226	OA Bipolar	1000	400	5-36	7 × 3	2,6	25dB stable
OPA699	OA Bipolar	1000	1400	5-12	22,5 × 3	4,1	12dB stable
OPA2354	OA CMOS	250	150	2,7-5,5	7,5 × 3	6,5	
INA2331	Instrumentation CMOS	50	5	2,5-5,5	0,5	46	
INA103	Instrumentation BIPOALR	80	15	9-25	9	1	

III. High performances analog frequency filters



Motivation

- ❖ Correct **analog** processing close to the physical sensor is the best way to condition the signal
- ❖ Noise is still based on the **reduction of the spectrum** (Lock-in, FFT ...)
- ❖ Frequency filters: **crucial block**

- ❖ → Objectives:
 - Optimization of the dynamic range (attenuation)
 - Mastering of the topic, related work not presented in the thesis (goal-lossy active filters [*], adaptive analog signal processing [**), microwave superconductor filters [***)

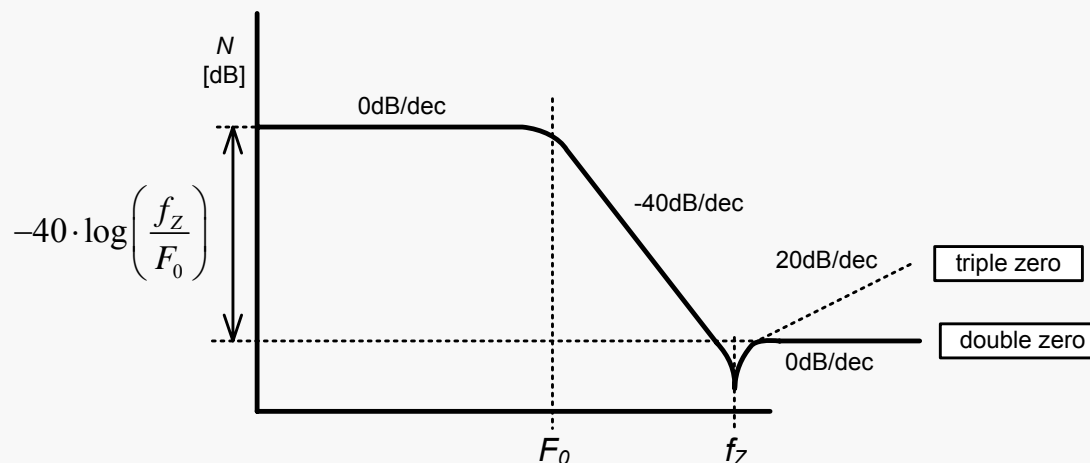
[*] V. Michal et al. "Active filters based on goal-directed lossy RLC prototypes", Speto int conference (2006)

[**] V. Michal et al. "The analog Filter Design and Interactive Analog signal Processing by PC" WSEAS (2005)

[***) V. Michal et al. "Superconducting NbN band-pass filter and Matching circuit for 30GHz RSFQ Data Converters ", IEEE conference Radioelek, 2009

Real-world frequency filters

- Non-ideal passive components:
 - F_0, Q inaccuracy, higher order effects, can be compensated [*]
- Non ideal active components
 - F_0, Q inaccuracy, DC offset, [attenuation](#)



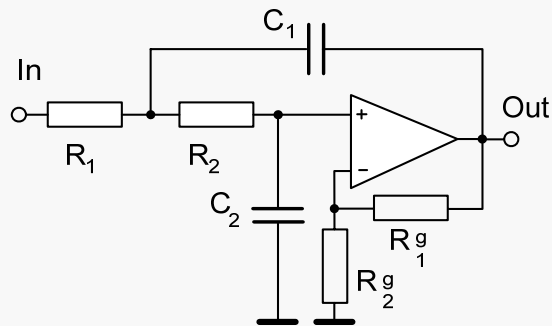
Parasitic zeros can not be compensated by predistortion [**]

Effect of parasitic zeros in the AC response of frequency filter

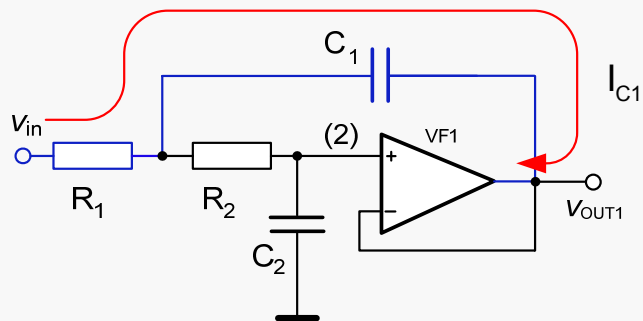
[*] Geffe, P. R., IEEE Trans., Vol. CAS-23, pp.45-55, 1976

[**] see: "Stop-band limitations of the Sallen-Key low-pass filter", AN Texas instrument, see also Schmid, H. Moschytz, G.S, Circuits and Systems, vol.1, 1998, p. 57-60.

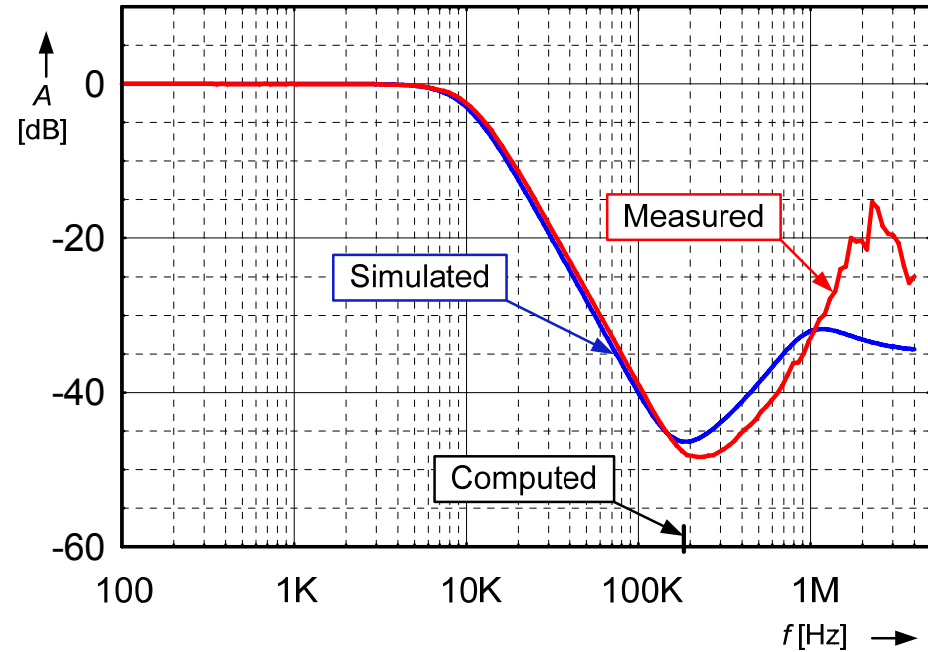
Example: real Sallen-Key filter



LP Sallen-Key biquad [*]



parasitic transfer zeros in the stopband

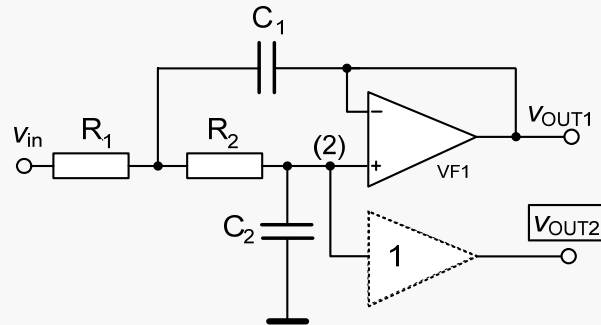


Parasitic zero occurs at :

$$f_z = \frac{1}{2\pi} \sqrt[3]{\frac{2\pi GBW}{R_0 R_2 C_1 C_2}}$$

[*] Sallen.R.P-Key.E.I., Circuit Theory. Vol. 7. 1955, p. 74-85.

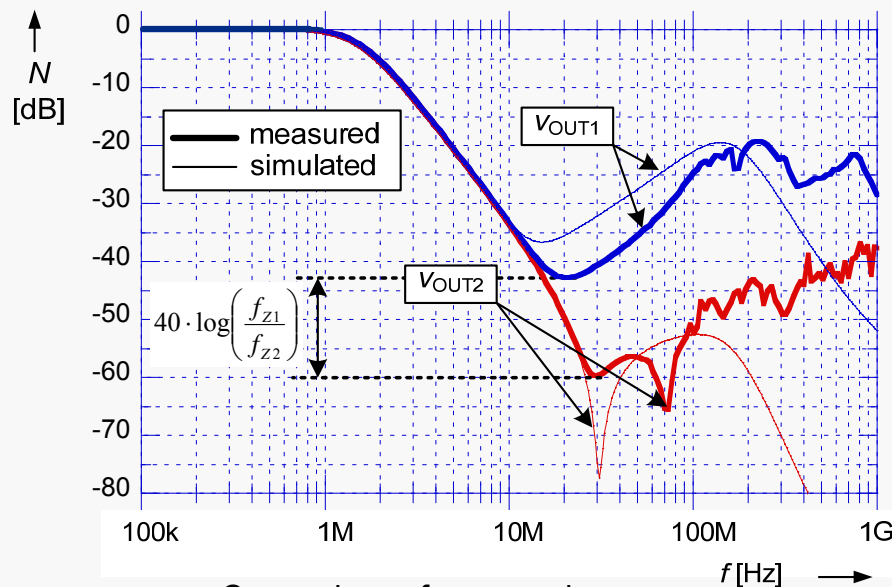
Real Sallen-Key: compensation



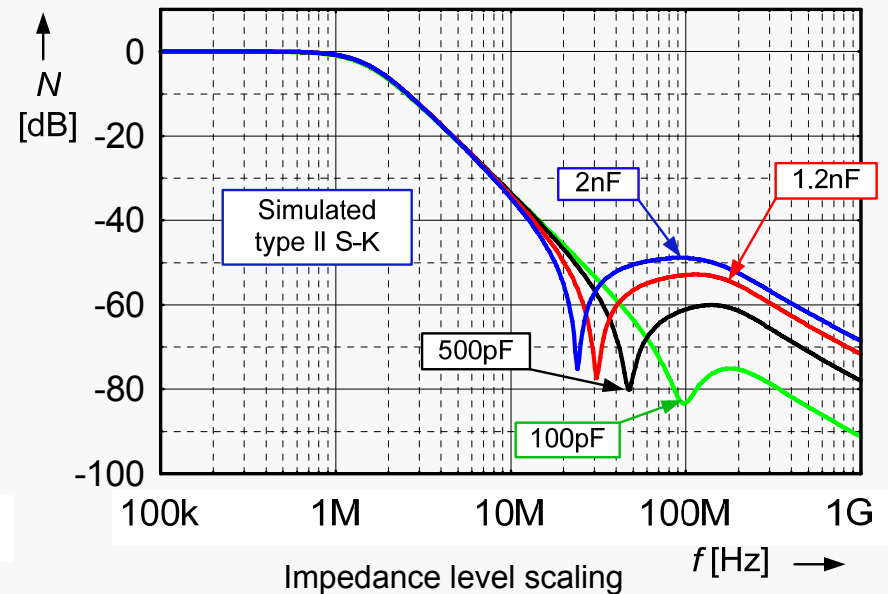
$$f_{Z(2)} \cong \frac{1}{2\pi} \sqrt{\frac{A \cdot \omega_p}{C_1 R_{OUT}}}$$

reduced order of the root,
only R_{out} and C_1 contribute to the
frequency \rightarrow **Higher attenuation**

Improved Type II Sallen-Key



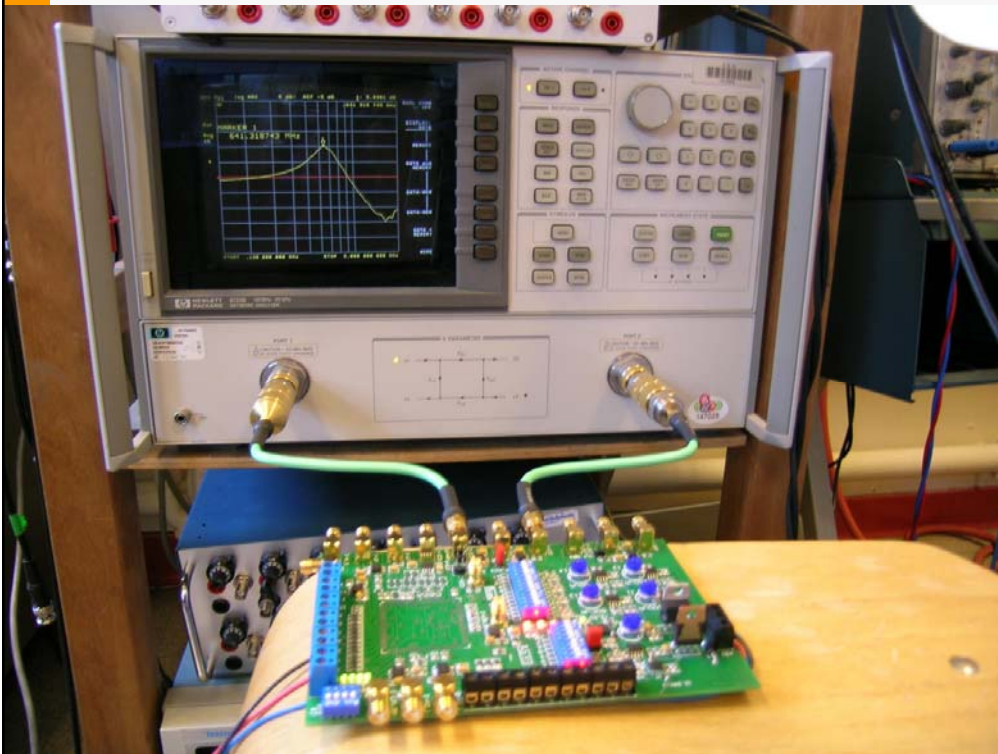
Comparison of v_{OUT1} and v_{OUT2}



Impedance level scaling

III.1

CCII biquadratic section



Proposed solution

Removal of the parasitic zeros ensure [constant -40db roll-off](#)

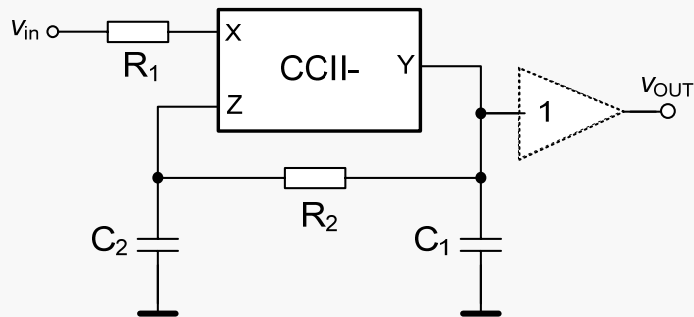
- Division of the frequency band in two regions:
 - **region up to f_0** , whereas the DC transfer and resonance gain is ensured by the active element
 - **region stop-band**, where the high attenuation is ensured by the passive RC filter

- **Design rules:** Interruption of direct signal way,
Passive filters containing grounded capacitors

[Adopted solution](#): topological transformation of circuits presented in [*]

[*] Liu, S-I., Tsao, H-W; Wu, J., Tsay, J-H. "Realizations of the single CCII biquads with high input impedance", IEEE Symposium on Circuits and Systems, 1991.

New biquadratic section CCII-

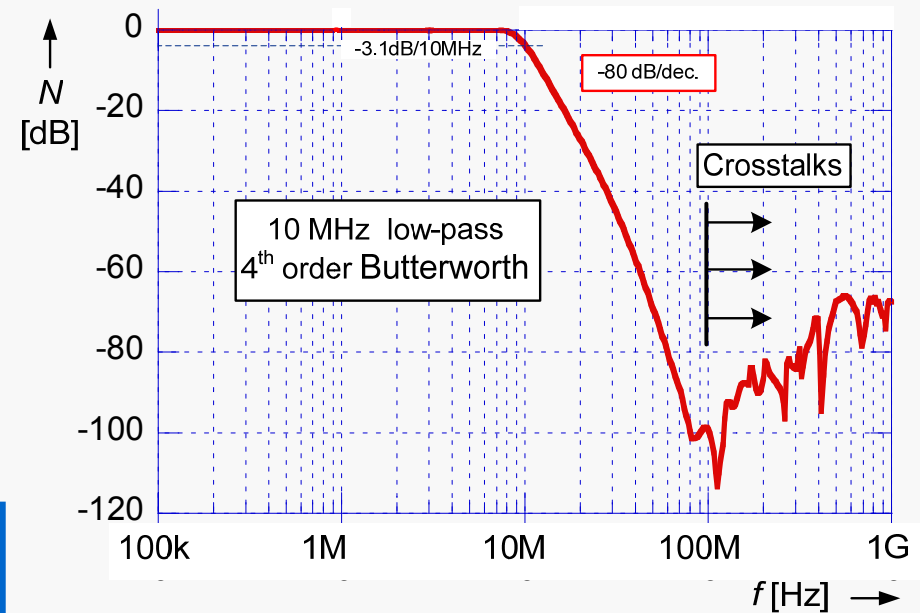


CCII- low-pass biquadratic section with eliminated parasitic transfer zero

Stop band behavior (single pole model of CCII):

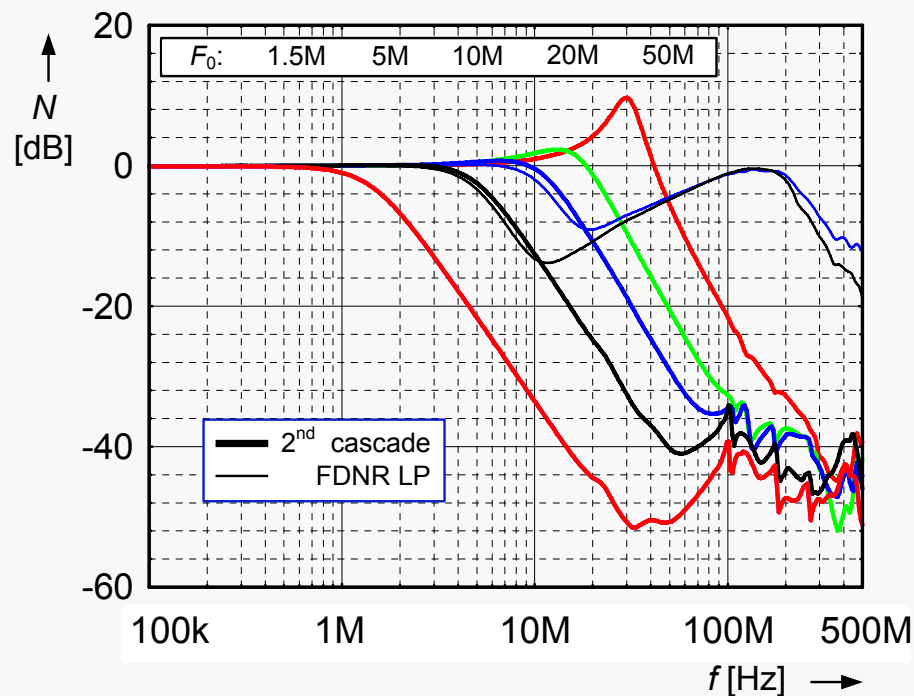
$$H(s) = \frac{\Omega_0^2}{(s^2 + s \cdot \Omega_0 / Q_0 + \Omega_0^2)} \cdot \frac{(\omega_p \cdot A_0 + s)}{(\omega_p \cdot (1 + \alpha) \cdot A_0 + s)}$$

$$f_0 = \frac{1}{2\pi\sqrt{R_1 R_2 C_1 C_2}} \quad Q = \frac{\sqrt{R_2}}{\sqrt{R_1}} \cdot \frac{\sqrt{C_1 C_2}}{C_1 + C_2} = \frac{1}{2} \cdot \sqrt{\frac{R_2}{R_1}} \Big|_{C_1=C_2}$$



measured AC response of 10MHz 4th order LP filter

Summary of achieved features



*Attenuation floor independent on the f_0 .
comparison with lossy R-FDNR biquad [*]*

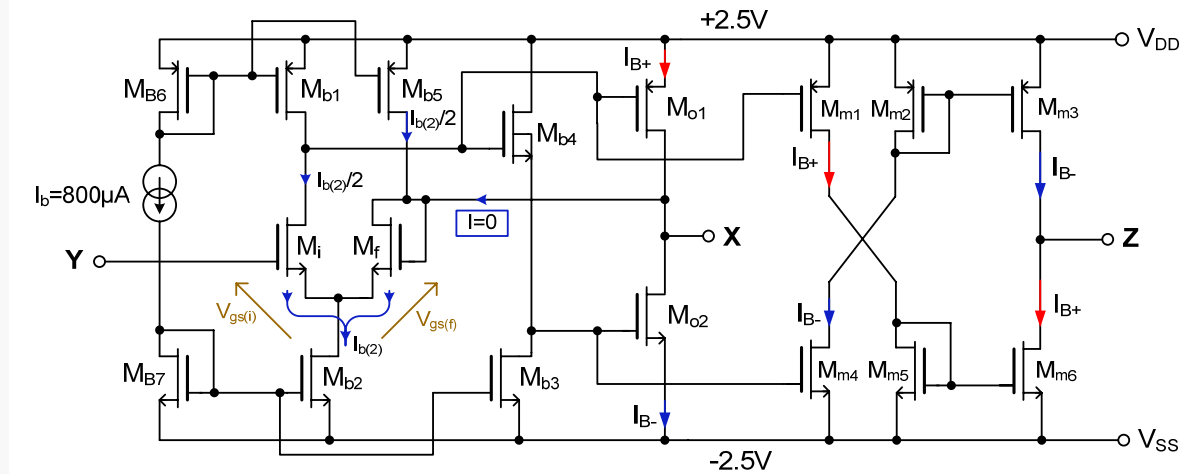
- The attenuation is only limited by signal leakage
- Does not depend on the f_0
- Using low-performance voltage buffer is allowed
- Direct connection to the DAC input
- ➔ price and consumption are reduced

[*] Martinek, P. , Proceeding of Radioelek, 2008

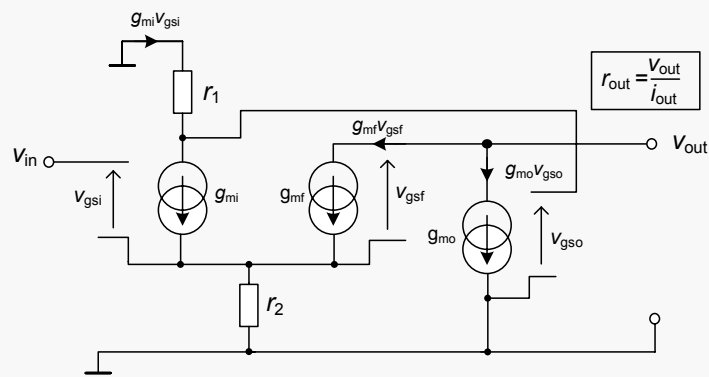
III.2

High performances CCII current conveyor

Design of Ultra-low R_{out} CCII-



CCII- with very low output resistance voltage buffer

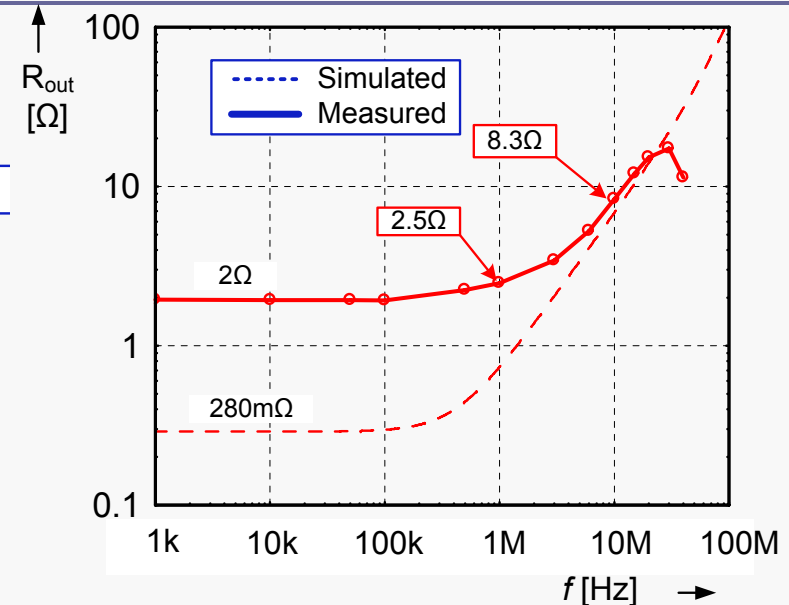
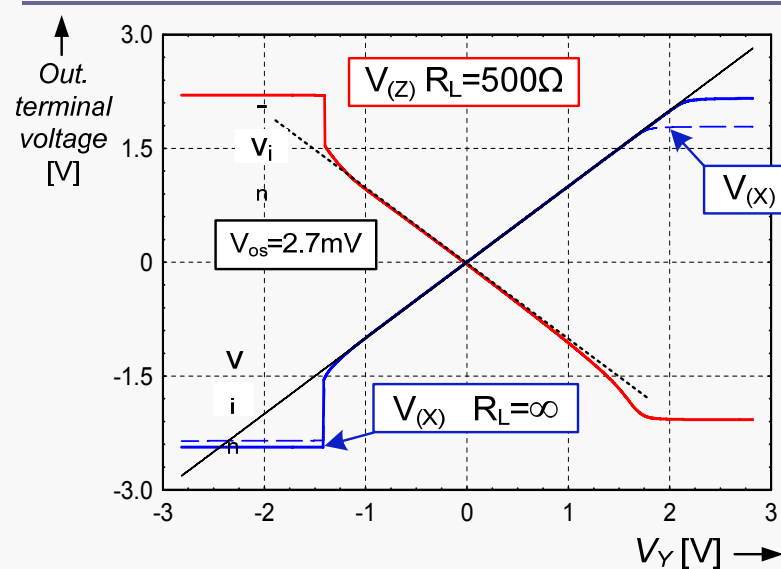


simplified small signal model

$$r_{out} = \frac{v_{out}}{i_{out}} = \frac{2 \cdot r_2 + 1}{r_2 \cdot g_{mf} + r_1 \cdot r_2 \cdot g_{mo} \cdot g_m + g_m}$$

$$\approx \frac{2}{r_1 \cdot g_{mo} \cdot g_m} \Rightarrow 0$$

Global performances: state of the art



V_{DD}	+/- 2.5V
Quiescence current	11 mA
Port X,Z voltage swing	+/- 1.5 V
Port X,Z driving capacity	+/- 20 mA
Port Z DC impedance	~7.5 M Ω
Port X offset voltage	2.7 mV
Port Z offset current	2.25 μ A
-3dB AC transfer Y \rightarrow X	~110 MHz
Port X resistance @ DC	2 Ω
Port X impedance @ 1MHz	2.5 Ω
Port X impedance @ 10MHz	8.5 Ω

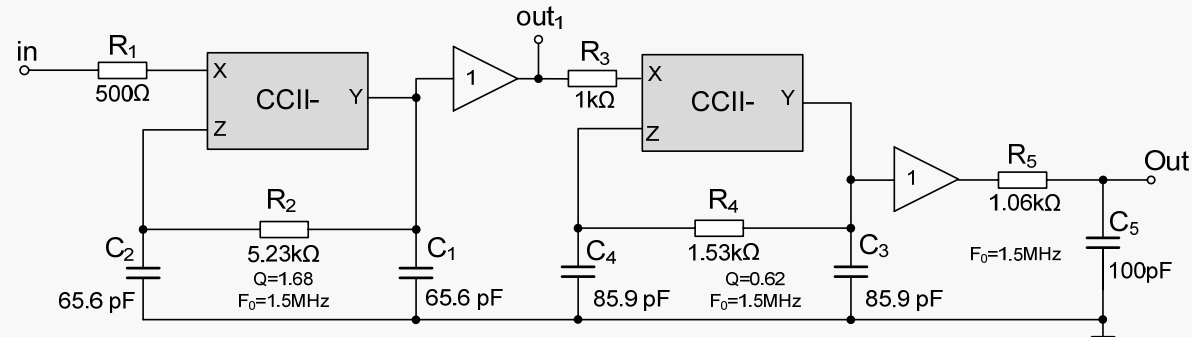
Summary of achieved performances

Recently published results on UVC [*]:

terminal	10kHz	1MHz	10kHz
z+	2.1 Ω	10 Ω	89 Ω
z-	0.9 Ω	8.2 Ω	76k Ω

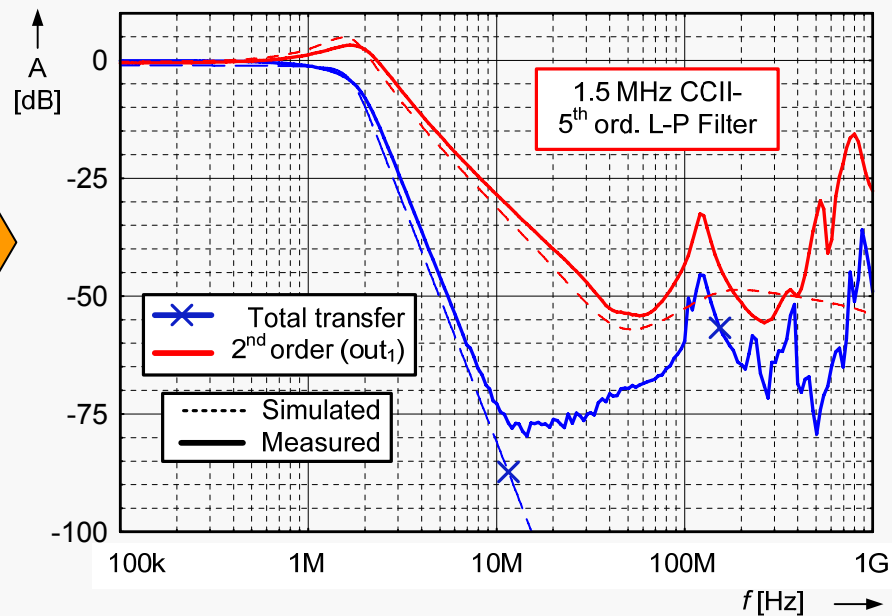
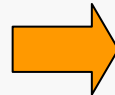
[*] Minarcik, M., Vrba, K. ICN'07

Experimental result: 1.5MHz LPF

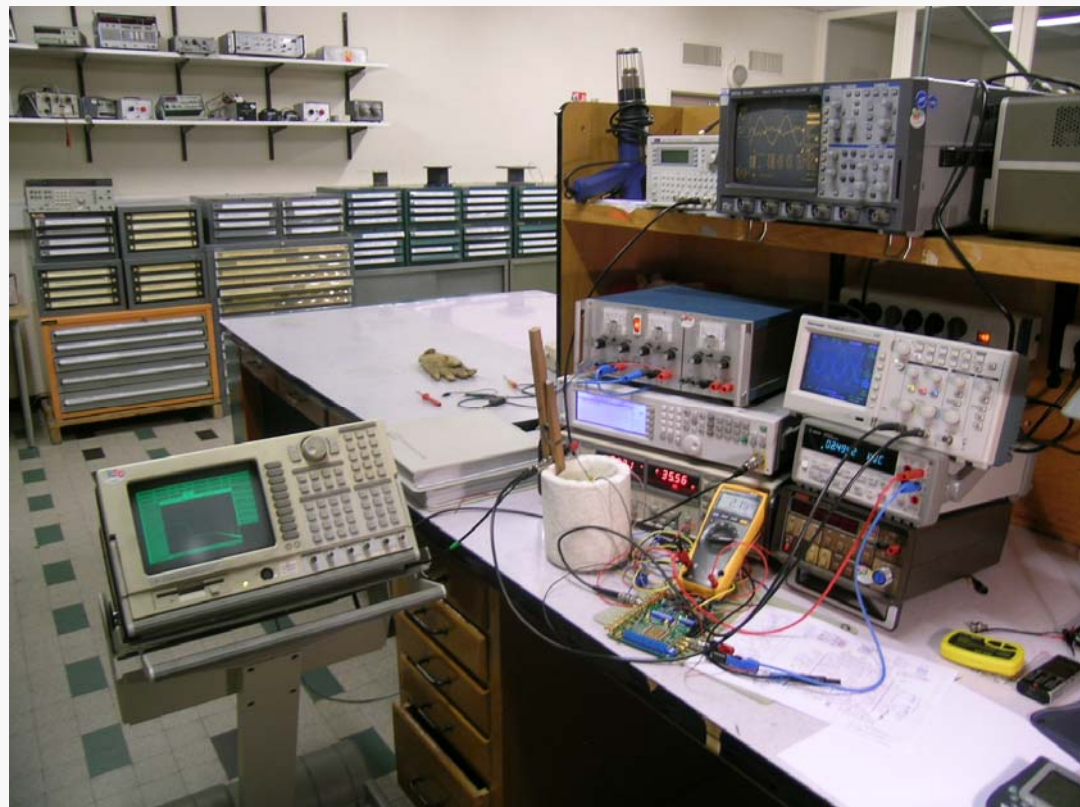


5th order LP filter (Butterworth) using new CCII biquadratic section

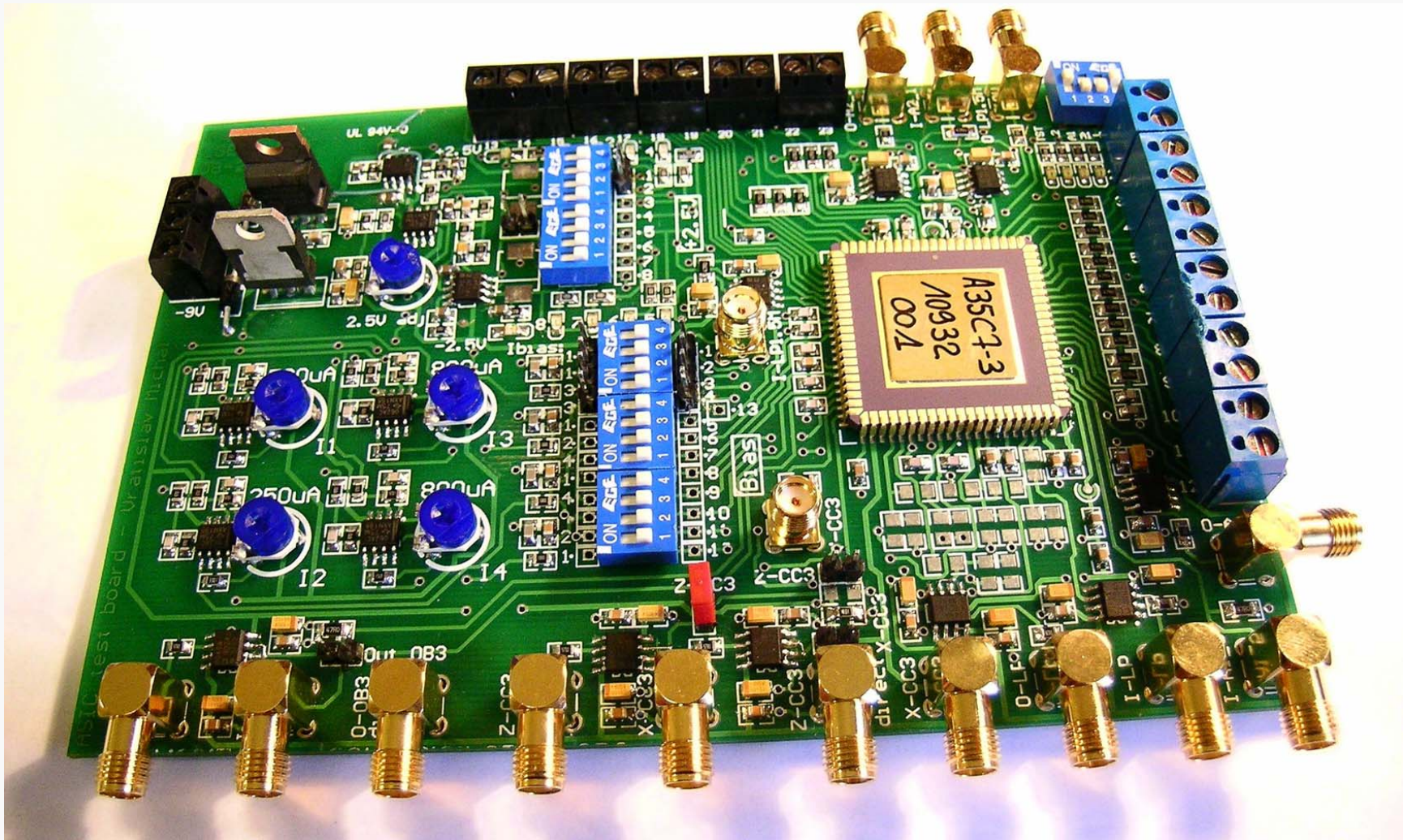
characteristic of 1.5MHz
5th ord. LP filter



IV Summary



Summary: example of test facility



Conclusion: scientific contribution

New generation of differential (instrumentation) amplifiers

Feedback-free architecture. State-of-the-art of the performances, competitives with the bipolar technology: High BW, low power consumption, low noise level

Cryogenic instrumentation, innovants design approaches

Analytical thermal model of the MOS, hybrid voltage-current biasing method

Analog front-end circuits optimizing

New structures with improved behavior in stop-band, large extension of band-width

Fabricated circuits ready to use in the new generation THz detector test set-up

Perspectives: Integration of the electronic in the THz test-bench

Implementation of designed circuits in industrial applications

French

Corrections..

Thank you

This research project has been supported by a Marie Curie Early Stage Research Training Fellowship of the European Community's Sixth Framework Program under contract number MEST-CT-2005-020692, and by the Grant Agency of the Czech Republic under Grant 102/03/1181.

